Thanks for the editor and reviewers for the comments to improve the quality of our manuscript. We have carefully addressed the comments with point-by-point replies to the reviewers and also Dr. Zeli Tan and revised our manuscript accordingly. Attached is a marked-up version of the manuscript.

Responses to the reviewer #1:

We thank the reviewer #1 very much for the valuable comments on our manuscript. The comments (bolded) are fully addressed as follows.

The manuscript presents results of introducing "K profile" parameterizatioin of turbulence into lake module of Community Land Model. This is likely the first time K profile parameterization is used in a 1D lake model, though it is widely applied in ocean models. Incorporation of new turbulence closure instead of standard Henderson-Seller diffusivity lead to significant improvement of simulation of late-summer destratification event in an Alaskan lake.

General comment

My general comment on the manuscript is that since single mixing event is simulated, more physical analysis could be provided to explain why K profile closure performed better than Henderson-Sellers in this case. Analysis presented in sections 3.1 and 3.2 is superficial and does not touch this question. One mixing case is not enough to state that K profile is better in similar situations in general, so more substantial inquiry into physics behind both parameterizations is needed. The authors state that KPP includes effects of thermal forcing, whereas original scheme of CLM model does not. This is actually not correct. First, original CLM model includes convective adjustment scheme (Subin et al., 2012) which instantaneously mixes the unstably stratified water column. Then, the effects of stable stratification are included via Brunt-Vaisala frequency in Henderson-Sellers (H-S) diffusivity. Thus, thermal (density) stratification is taken into account. The mixing event the authors focus on happens during weakly stable stratification under strong wind forcing. One may conclude from simulation results presented is that given the same stable temperature profile the larger wind speed is needed for H-S to mix completely the water column than for KPP model. This may be elaborated by conducting idealized simulations with both turbulence closures with varying wind speeds and temperature profiles where this statement may be checked and respective quantitative estimates provided.

Response: Thank you for the insightful comments. We modified several places in the manuscript to address your questions. Our general reply is as follows.

The difference of the current mixing parameterization of the CLM (CLM-ORG) and the KPP (CLM-KPP) is in the equations used to estimate eddy diffusivity. In CLM-KPP, the eddy diffusivity is estimated separately for the lake boundary layer and lake interior. In the lake boundary layer, the eddy diffusivity is not determined by local gradient of mean variables, but it is determined by surface forcing and the boundary layer depth. The non-local effect is taken into account by estimating the boundary layer depth first, and the eddy diffusivity is specified with a prescribed profile in the boundary layer. In the lake interior, the mixing is generally weak and associated with internal wave activity and shear instability. From our point of view, the major shortcomings of CLM-ORG are that it does not consider a boundary layer for eddy development, and it requires an ad hoc parameter to enhance the estimated eddy diffusivity. In the KPP scheme, an explicit inclusion of an ad hoc enlarging parameter is avoided. The KPP scheme was tested for different time scales, diurnal change, seasonal cycle, and single event for different locations (Large et al. 1994). We have also conducted more simulations for other lakes with quite different environment settings, e.g. Nam Co at Tibetan Plateau with a focus on its long term change, and the results are presented below.

For Nam Co, located in the Tibetan Plateau, we conducted simulations at a 10-km spatial resolution over the period of 2003 through 2012. Our simulations showed that the lake WST simulations with CLM-KPP were significantly improved when compared with CLM-ORG simulations. We have added simulations and analysis for Nam Co to the manuscript:

"We validated both CLM-ORG and CLM-KPP with the monthly Moderate Resolution Imaging Spectroradiometer (MODIS) data for Nam Co by conducting 10-km spatial resolution simulations for this lake over the period of 2003 through 2012. We can see that CLM-KPP improved WST simulations averaged over the entire lake (34 model grid cells) when compared with the CLM-ORG simulations (Fig. R1). The RMSE of WST decreased from 4.58 ˚C with CLM-ORG to 2.23 ˚C with CLM-KPP, and the R increased from 0.90 to 0.96 at the same time.

The differences in the mixing coefficients of CLM-KPP and CLM-ORG cause the difference in WST simulations. We averaged the K_w^{ORG} and K_w^{KPP} over the water columns with the depth greater than 25 m for Nam Co (Fig. R2), and the total of such columns were 28 out of 34 for this lake. Figure R2 indicated that K_w^{KPP} was slightly smaller than K_w^{ORG} mostly in the mixed layer of the lake during summer time. In the deeper part of the lake, K_w^{KPP} was much smaller than K_w^{ORG} during summer time. In the spring and fall seasons, K_w^{KPP} was significantly larger than K_w^{ORG} where the buoyancy flux may contribute strongly to K_w^{KPP}. During the winter time when the lake froze, both CLM-KPP and CLM-ORG were set to use K_w^{ORG}. We can see that the most significant improvements in WST for Nam Co occurred during the ice-free seasons when the KPP was activated."

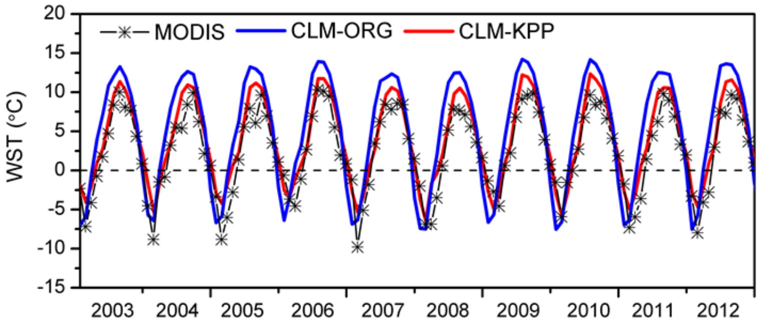

Figure R1. Time series over the period of 2003 through 2012 of monthly WST observations from MODIS (black starred line) and simulations with CLM-ORG (blue line) and CLM-KPP (red line) (Unit: ˚C).

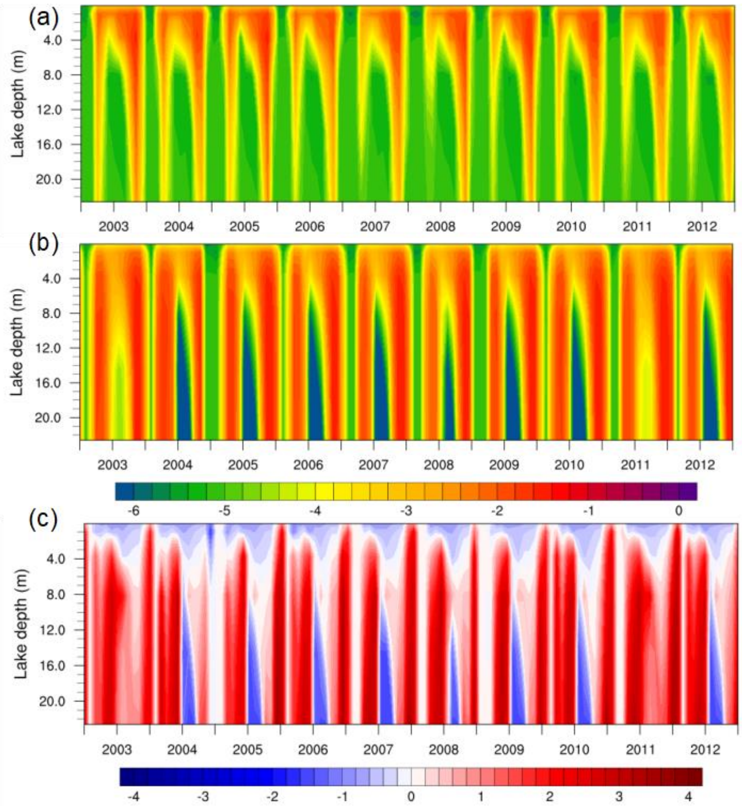

Figure R2. Simulated (a) $log_{10} K_w^{ORG}$ with CLM-ORG, (b) $log_{10} K_w^{KPP}$ with CLM-KPP (Unit: m^2/s) averaged over water columns with depth greater than 25 m (28 of 34 grid cells), and (c) differences between $log_{10} K_w^{KPP}$ and $log_{10} K_w^{ORG}$ ($log_{10} K_w^{KPP} - log_{10} K_w^{ORG}$).

In CLM-KPP, the eddy diffusivity formulation is different for the boundary layer and lake interior. In the lake boundary layer, the eddy diffusivity is related with boundary layer depth and surface forcing. In the lake interior, the eddy diffusivity is relatively weak, associated with internal wave activity and shear instability. Overall the CLM-KPP can enhance the eddy diffusivity during spring and fall and maintain weak eddy diffusivity in the lake interior during summer when stratification is strong. The outcome of the CLM-KPP eddy diffusivity is an improved WST simulation.

For Fog3 Lake in Alaska, numerical experiments were conducted for CLM-ORG with enhanced wind. Figures R3 and R4 showed simply providing larger winds could not significantly improve CLM-ORG simulations for this lake (Table R1).

When stronger wind is used, the CLM-ORG can simulate the mixing event around 16 Aug. However, the strong wind causes WST to have a negative bias, presumably caused by heat loss from the lake. Thus, as shown in the manuscript, the CLM-KPP provides a better parameterization of eddy diffusivity and improved lake temperature simulations.

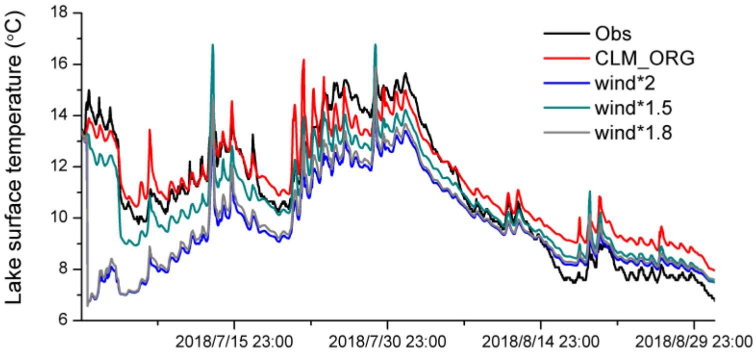

Figure R3. WST observations (black line) and CLM-ORG simulations with the default wind data (red line), with wind data 2-fold increased (blue line), with wind data 1.5-fold increased (green line), and with wind data 1.8-fold increased (grey line) (unit: ˚C).

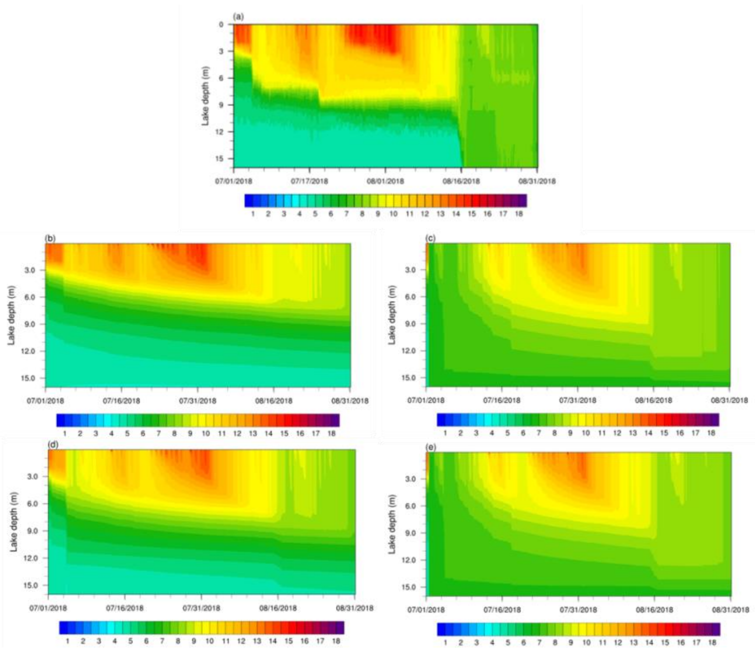

Figure R4. Lake temperature profiles of (a) observations and CLM-ORG simulations with (b) the default wind data, (c) with wind data 2-fold increased, (d) with wind data 1.5-fold increased (green line), and (e) with wind data 1.8-fold increased (grey line) (unit: ˚C).

Table R1. RMSE (˚C) and R of the temperature profile simulations with CLM-ORG, the case with wind 2-fold increased, the case with wind 1.5-fold increased, and the case with wind 1.8-fold increased for Fog3 Lake for the periods of 1 July–15 August and 16–31 August 2018.

	1 July–15 August, 2018		16–31 August, 2018	
	RMSE (˚C)	R	RMSE (˚C)	R
CLM-ORG	1.1	0.93	1.4	0.57
wind×2	2.0	0.83	0.5	0.63
wind×1.5	0.83	0.97	1.1	0.59
wind×1.8	2.0	0.84	0.6	0.62

We also mentioned the convective adjustment scheme in the manuscript. The convection scheme works when there exists density instability (Hostetler and Bartlein, 1990).

Specific comments

(1) Lines 88-90: "Researchers have attempted to advance this lake model to more closely reflect reality over the last two decades (Fang and Stefan, 1996; Henderson-Sellers, 1985; Hostetler and Bartlein, 1990; Subin et al., 2012)." Three of four papers cited here do not deal with CLM model.

Response: We deleted this sentence.

(2) Lines 92-93: "... is the enhanced eddy diffusivity for unresolved mixing processes". All mixing processes in 1D model are unresolved and are parameterized, because only 3D model of sufficiently high resolution simulates turbulence explicitly.

Response: We agreed with this reviewer on this comment. We changed "for unresolved mixing processes" to "to strengthen mixing processes" (Page 3 Line 15)

(3) Line 98: "0.0012u_2" I guess, you can write drag coefficient C_d instead of 0.0012, to make the physical sense of this equality clear.

Response: Yes, we changed "0.0012" to "C_d" in the manuscript (Page 3 Line 22 and Eq. (3)).

(4) Eq. (5): please separate this fraction into two.

Response: Yes, we separated the fraction into two parts (Page 4 Eq. (6)).

(5) Section 2.1.1: you didn't mention convective adjustment scheme in CLM lake model. It should work during nights

in your simulation.

Response: Yes, based on the general comment, we included convective adjustment scheme to the manuscript (Page 3 Line 11 to Line 12).

(6) Section 2.2: too concise description of the lake. Put more info on climate and landscape conditions, hydrological regime, previous research of the lake.

Response: Yes, we added more description of Fog3 Lake to the manuscript:

Change "Fog 3 Lake, is in Arctic Alaska at (68.67˚ N, 149.10˚ W) (Fig. 1a). In 2018 it had a surface area of 35,230 m^2 and a maximum depth of 19.74 m. The lake has a long ice duration, and ice-off is usually in late June, while ice-on typically occurs in early October (Arp et al., 2015)."

to

"Fog3 Lake is in Arctic Alaska at (68.67˚ N, 149.10˚ W) (Fig. 1a). In 2018 it had a surface area of 38,863 m^2 and a maximum depth of 21 m. The lake has a long ice duration, and ice-off is usually in late June, while ice-on typically occurs in early October (Arp et al., 2015). Around this lake, the mean annual air temperature is about ~ –6 ℃, and the mean annual precipitation is ~ 200 mm (Ping et al., 1998). This kettle lake is surrounded by lower hills covered mainly with shrubs and tundra. Due to the treeless landscape, there are no shielding effects on the wind. In addition, Fog3 Lake is formed by glaciers, and has less connection to other surrounding surface waters." (Page 6 Line 6 to Line 12).

(7) Line 154: "wind-only driven scheme". Again (see above), it is incorrect to state that basic CLM lake model includes only wind forcing, as it accounts for both stable and unstable stratification.

Response: Yes, see the response for the general comment.

(8) Section 2.3: I would add more info on the organization of measurements. Is there a mast on a lake? Which organization runs measurements? Any relevant references?

Response: Fog3 Lake is about 1.5 km from Toolik Field Station (68°37.796' N, 149°35.834' W), in the northern foothills of the Brooks Mountain Range, Alaska (https://toolik.alaska.edu/edc/abiotic_monitoring/index.php) (Page 6 Line 18 to Line 20).

(9) Line 173: "estimates a stratified lake": sounds badly, please rephrase.

Response: Yes, we changed this sentence to **"**CLM-KPP accurately captured the mixing event (Fig. 3c), while CLM-ORG produced strong stratification in the upper part of the lake throughout the simulation period (Fig. 3b)**"** (Page 7 Line 28 to Line 29).

(10) Table 1 is too small, you can easily present those numbers directly in text.

Response: We separated our entire simulation period for Fog3 Lake into the before and after mixing periods and calculated RMSE and R for these two periods (Table R2; Table 1 in the manuscript). We can see that CLM-KPP remarkably improved the water mixing simulations in Fog3 Lake when compared with CLM-ORG.

Table R2. RMSE (˚C) and R of the temperature profile simulations with CLM-ORG and CLM-KPP for Fog3 Lake for the periods of 1 July–15 August and 16–31 August 2018.

	1 July–15 August, 2018		16–31 August, 2018	
	RMSE (˚C)	R	RMSE (˚C)	R
CLM-ORG	1.1	0.93	1.4	0.57
CLM-KPP	1.3	0.92	0.3	0.99

(11) Lines 183-184: "Thermal forcing played a vital role in this enlarged diffusivity, which was considered only in CLM-KPP and not in CLM-ORG." See my comment 7 above and general comment.

Response: Yes, see the response for the general comment.

(12) Line 188: "10^{-7}" please put units and elsewhere in the document.

Response: Yes, we put units and elsewhere in the manuscript (Page 8).

(13) Line 188: "was the product" It is not product, but a sum.

Response: Yes, we changed "product" to "sum" in the manuscript (Page 8 Line 11).

(14) Lines 198-201: two sentences, stating almost the same.

Response: The first sentence states N^2, while the second sentence states the water stratification (Page 8 Line 18 to Line 21).

(15) Line 238: "absorbed solar radiation". It is radiation flux.

Response: Yes, we modified "absorbed solar radiation" to "radiation flux" in the manuscript (Page 11 Line 3).

(16) Lines 239-240: "total eddy diffusivity". Better: total diffusivity.

Response: Yes, we modified "total eddy diffusivity" to "total diffusivity" in the manuscript (Page 11 Line 4).

(17) Eq. (A3): a0, a1, ... Better to put numbers into subscript (a_0, a_1, ...).

Response: Yes, we put numbers into subscript accordingly in the manuscript (Page 11 Line 7).

(18) Eq. (A4) (both equations): there is a derivative sign in numerator and not in denominator.

Response: Yes, we made it more clearly in the manuscript (Page 11 Line 8 to Line 10).

(19) Line 244: Not clear, what is $\vartheta(h)$? You say, it is "water diffusivity". But, water diffusivity is K_w. There are also molecular diffusivity, background diffusivity, diffusivity caused by internal waves … all denoted differently above.

Response: $\vartheta(h)$ refers to the total diffusivity of water, a sum of molecular diffusivity, background diffusivity, diffusivity caused by internal waves. We made it more clearly in the manuscript (Page 11 Line 8).

(20) Line 246: replace "buoyancy difference" by "buoyancy".

Response: Yes, we replaced "buoyancy difference" by "buoyancy" in the manuscript (Page 11 Line 11).

Responses to the reviewer #2:

We thank the reviewer 2 very much for the valuable comments on our manuscript. The comments (bolded) are addressed below.

First, thank you for sharing your work. This is a very interesting study! You present a method of improving the thermal mixing of lakes in the Community Land Model (CLM). The new method introduced into CLM is K profile parameterization (CLM-KPP), a method utilized in ocean modeling. The current CLM vertical mixing scheme (CLMORG) assumes wind is the primary forcing in thermal mixing of lakes. KPP uses wind and surface thermal forcing to simulate lake temperatures. The model did not improve until a mixing event occurred on 16-31 August. CLM-ORG predicted a continued stratification of lake temperature from 16-31 August. CLM-KPP correctly estimated when and the magnitude at which the thermal mixing event would occur from 16-31 August. You provide a thorough analysis as to how thermal forcing within CLM-KPP was able to correctly predict that the mixing would occur. However, I believe there a couple of points that would enhance this work.

Major Comments 1. The study seems limited using only one lake and a very narrow time frame. I would recommend the inclusion of several study locations and/or a longer period of analysis to get a better sense of the implications of using CLM-KPP over CLM-ORG. Right now the impact of the study feels limited given that only one location is examined for a two month period during the same season.

Response: We chose another lake, Nam Co, to evaluate CLM-ORG and CLM-KPP. We validated both CLM-ORG and CLM-KPP with the monthly Moderate Resolution Imaging Spectroradiometer (MODIS) data for Nam Co by conducting 10-km spatial resolution simulations for this lake over the period of 2003 through 2012. We can see that CLM-KPP improved WST simulations averaged over the entire lake (34 model grid cells) when compared with the CLM-ORG simulations (Figs. R1 and R2). The RMSE of WST decreased from 4.58 ˚C with CLM-ORG to 2.23 ˚C with CLM-KPP, and the R increased from 0.90 to 0.96 at the same time. We have added simulations and analysis for Nam Co to the manuscript.

2. Related to 1, you do not provide an analysis of how the stratification beginning on 16 Aug better informs ecosystem, meteorological, or climatological analysis for the lake. A better discussion of implications of capturing this mixing, particularly if any were observed, would enhance this work.

Response: Stratification plays an important role in lake production and food webs. Stratification and warmer epilimnion temperatures create conditions necessary for phytoplankton production. Also, when Arctic lakes become strongly stratified, the hypolimnion can become anoxic, which in turn increases nutrient recycling and leads to elevated production the following spring (O'Brien et al., 2005). Increased food availability and warmer lake temperatures in the epilimnion from stratification increase arctic char growth. Finally, simulations of stratification date and epilimnion temperature are used in bioenergetic models to estimate fish growth and consumption and better understand Arctic char production with global environmental change (Budy and Luecke, 2014) (Page 2 Line 6 to Line 12).

3. Line 169-180: You discuss how RMSE and correlation (R) improved with CLM-KPP only slightly for the entire simulation period. I suggest that since you use these metrics, divide the calculation of these metrics into a before and after the mixing event occurs. This would strengthen your point. You should then note this in the abstract and conclusions to better illustrate the impact that CLM-KPP has in the simulation.

Response: Based on this comment, we separated our entire simulation period for Fog3 Lake into the before and after mixing periods and calculated RMSE and R for these two periods (Table R2; Table 1 in the manuscript). We can see that CLM-KPP remarkably improved the water mixing simulations in Fog3 Lake when compared with CLM-ORG.

Minor comments

Line 100: Please define phi.

Response: Actually, we define phi (φ) in Page 3 Line 22 "k^* is related to latitude φ" in the manuscript.

Line 161: How did you decided upon the 24 layers you specify?

Response: The depth for this lake was set at 20 m in both models. Observed lake temperatures for Fog3 Lake are for lake depths of 0, 1, 2, 3, 4, 5, 6, 7, 8, 10, 12, 14, and 16 m. The lake model has 10 lake layers by default, and the center point depths of these layers are 0.05, 0.3, 0.9, 1.9, 3.3, 5.1, 7.5, 10.3, 13.79, and 17.94 m generated automatically by the layering scheme in the model based on the input lake depth. For this study, we tried to keep each layer thin in the top part of the lake to reflect diurnal cycles (layers 1–5) in both CLM-ORG and CLM-KPP. Below layer 5, we used mostly the observed points to layer the rest of the lake column. Finally, we produced 24 layers for the entire lake column in both models, and the center point depths of these lake layers are 0.05, 0.15, 0.25, 0.35, 0.45, 1, 2, 3, 4, 5, 6, 7, 8, 9, 10, 11, 12, 13, 14, 15, 16, 17, 18, and 19.25 m, respectively (Page 7 Line 8 to Line 15). As shown in the Fig. R5 and Table R3, the simulations of CLM-ORG with both 10 and 24 layers were very similar, while the simulations of CLM-KPP with 24 layers were closer to observations than those with 10 layers when the water mixing event occurred.

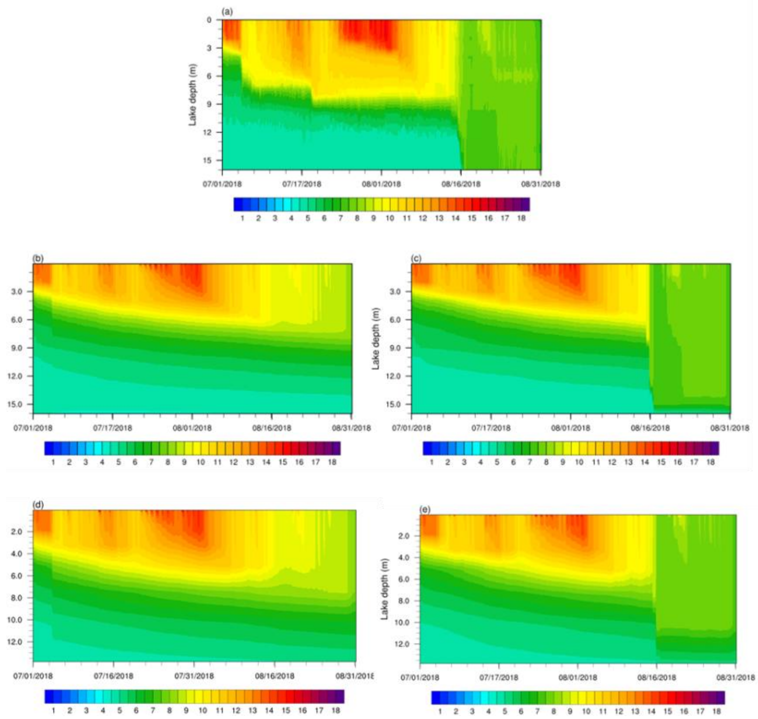

Figure R5. Lake temperature profiles of (a) observations, simulations of (b) CLM-ORG and (c) CLM-KPP with 24 layers and simulations of (d) CLM-ORG and (e) CLM-KPP with 10 layers (unit: ˚C).

Table R3. RMSE (˚C) and R of the temperature profile simulations of CLM-ORG and CLM-KPP with 10 and 24 layers for Fog3 Lake over the periods of 1 July–15 August and 16–31 August 2018.

		1 July–15 August, 2018		16–31 August, 2018	
		RMSE (˚C)	R	RMSE (˚C)	R
10 model layers	CLM-ORG	1.0	0.94	1.4	0.58
	CLM-KPP	1.2	0.94	0.7	0.90
24 model layers	CLM-ORG	1.1	0.93	1.4	0.57
	CLM-KPP	1.3	0.92	0.3	0.99

Responses to Dr. Zeli Tan:

We thank Dr. Zeli Tan very much for the constructive and helpful comments on our manuscript. The comments (bolded) from the reviewer Dr. Zeli Tan are fully addressed in the following.

It is an interesting study. Because a 1-D lake model is still much needed to understand the impact of climate changes on global lake systems, a parameterization method that could improve the simulation of lake mixing process will be much valued. But I suggest that the manuscript can be improved in the following directions. First of all, the comparison between CLM-ORG and CLM-KPP is not exhausted, to day the least. In Subin's CLM-ORG paper, he actually tested the model over a pair of lakes around the globe. In fact, the CLM-ORG performance on high-latitude lakes which this study focused on was not the worst. Thus, the method can become much more valuable if the authors can apply this method to some more lakes, especially those deep and large lakes.

Response: Thanks for the comments. We chose another lake, Nam Co, to evaluate CLM-ORG and CLM-KPP. We validated both CLM-ORG and CLM-KPP with the monthly Moderate Resolution Imaging Spectroradiometer (MODIS) data for Nam Co by conducting 10-km spatial resolution simulations for this lake over the period of 2003 through 2012. We can see that CLM-KPP improved WST simulations averaged over the entire lake (34 model grid cells) when compared with the CLM-ORG simulations (Figs. R1 and R2). The RMSE of WST decreased from 4.58 ˚C with CLM-ORG to 2.23 ˚C with CLM-KPP, and the R increased from 0.90 to 0.96 at the same time. We have added simulations and analysis for Nam Co to the manuscript.

Second, more information about the study lake is needed. Is Fog3 Lake a glacial lake or a thermokarst lake? How was the surface friction velocity derived for this lake? Are the effects of lake fetch and wind shielding considered? What is the lake's light attenuation coefficient?

Response: Fog3 Lake is a glacial lake. In CLM-ORG, the surface friction velocity w^* (m/s) is calculated as:

$$w^* = 0.0012u_2 \quad \text{(R1)}$$

where u_2 is the 2-m wind speed (m/s).

While in CLM-KPP, the surface friction velocity u^* (m/s) is calculated as (Large and Pond, 1982):

$$u^{*2} = \frac{\rho_a}{\rho} C_D U^2 \quad \text{(R2a)}$$

$$10^3 C_D = \frac{2.70}{U} + 0.142 + 0.0764U \quad \text{(R2b)}$$

where ρ_a and ρ are the air and lake water densities (kg/m^3) respectively, C_D is the drag coefficient and U is the 10-m wind speed (m/s). The effect of the lake fetch was considered in our simulations. In the CLM-ORG, the lake fetch F (m) (Hutchinson, 1957; Wetzel and Likens, 1991) is:

$$\mathrm{F} = \begin{cases} 100, & D < 4 \\ 25D, & D \geq 4 \end{cases} \qquad \text{(R3)}$$

where D is the water depth. We also used this function in CLM-KPP.

In this study, wind shielding was not considered. Actually, the Toolik meteorological station providing the wind data is ~1.5 km away from Fog3 Lake, although there are no buildings or trees between the Toolik station and the lake. Thus, the wind shielding effects are not significant. The light extinction coefficient η (m^{-1}) is a function of depth (m) (Hakanson, 1995):

$$\eta = 1.1925D^{-0.424} \qquad \text{(R4)}$$

In this study, with the lake depth (D) of 20 m for Fog3 Lake, η is about 0.33 m^{-1}.

Third, how are CLM-ORG and CLM-KPP calibrated in this study? I know that CLM-ORG has a water mixing parameter that can be used to increase diffusivity for those deep lakes. Can the parameter values of CLM-KPP described here be applied to other lakes?

Response: Both CLM-ORG and CLM-KPP were not calibrated in this study. Yes, the water mixing parameter in CLM-ORG can be increased to generate stronger water mixing for deep lakes (Gu et al., 2013). Here, we increased the water diffusivity (Eq. (1) in the manuscript) by 10 and 100 times in CLM-ORG and conducted additional simulations for Fog3 Lake as shown in Figs. R6 and R7. We can see that CLM-ORG was still unable to reproduce the observed lake temperatures with the enlarged water diffusivity. Again, we did not adjust any parameters in CLM-KPP when we performed simulations for Fog3 Lake, and the same parameters were applied to the simulations for Nam Co. We see that CLM-KPP more realistically captured the water mixing in Nam Co than CLM-ORG (Figs. R1 and R2).

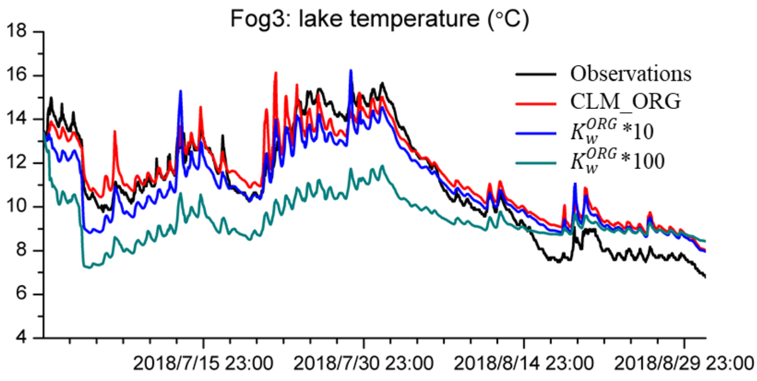

Figure R6. Lake WST observations (black line), simulations with CLM-ORG (red line), and simulations with K_w^{ORG} multiplied by 10 (blue line) and 100 (green line), respectively.

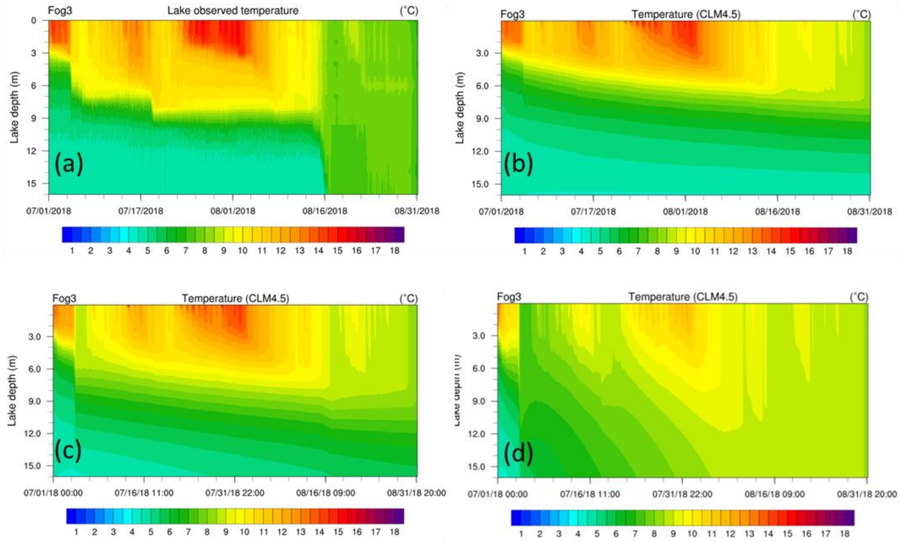

Figure R7. Lake temperature profiles of (a) observations, (b) simulations with CLM-ORG, and simulations with K_w^{ORG} multiplied by (c) 10 and (d) 100.

Forth, I am surprised that the case study did not cover the period of spring water mixing which can have large biogeochemical impacts for high-latitude lakes.

Response: Lake temperature data and some of the atmospheric forcing data for Fog3 Lake are available only for July and August 2018. However, our additional simulations with CLM-ORG and CLM-KPP for Nam Co covered the period of 2003-2012, which included the spring season (Figs. R1 and R2). Our simulations with CLM-KPP were closer to observations than those with CLM-ORG for almost the entire simulation period including the spring seasons.

Thanks for the authors to address my comments patiently. Overall, the response is great.

Just to remind that MODIS data is probably not good for lake model validation at specific lakes, especially at the spring and fall mixing periods when the rapid change of weather would introduce significant uncertainties (such as cloud cover). Thus, the uncertainty of MODIS data need to be acknowledged.

Responses: Yes, we acknowledged the uncertainties of MODIS data in the manuscript (Page 7 Line 2 to Line 5). Previous studies have verified MODIS WST data for lakes with *in situ* observations (Crosman and Horel, 2009; Schneider et al., 2009). Zhang et al. (2014) found that the nighttime WST of MODIS for Nam Co had a 0.89 correlation coefficient and a –1.4 ℃ bias when compared with surface observations. All these studies show that the MODIS WST has acceptable accuracy for studying lake thermal processes.

In addition, I do not think that the overestimation of surface temperature by CLM-ORG in summer is due to lack of mixing (Fig. R1). The other causes, such as the representation of latent and sensible heat, need to be acknowledged.

Responses: Yes, Figure R2 showed that K_w^{KPP} was slightly smaller than K_w^{ORG} mostly in the mixed layer of the lake during summer time. In the deeper part of the lake, K_w^{KPP} was much smaller than K_w^{ORG} during summer time. In the spring and fall seasons, K_w^{KPP} was significantly larger than K_w^{ORG}.

In CLM-KPP, the eddy diffusivity formulation is different for the boundary layer and lake interior. In the lake boundary layer, the eddy diffusivity is related with boundary layer depth and surface forcing. In the lake interior, water diffusivity is relatively weak, associated with internal wave activity and shear instability. Overall, CLM-KPP enhances the water diffusivity during the spring and fall and maintains weak water diffusivity in the lake interior during the summer when stratification is strong when compared to CLM-ORG. In addition, the overestimated WST with CLM-ORG before the summer affects the energy budget at the lake surface, which further influences lake temperature simulations during the summer.

References

Arp, C. D., Jones, B. M., Liljedahl, A. K., Hinkel, K. M., and Welker, J. A.: Depth, ice thickness, and ice-out timing cause divergent hydrologic responses among Arctic lakes, Water Resour. Res., 51, 9379-9401, https://dx.doi.org/10.1002/2015WR017362, 2015.

Budy, P., Luecke, C.: Understanding how lake populations of arctic char are structured and function with special consideration of the potential effects of climate change: a multi-faceted approach, Oecologia, 176, 81-94, https://dx.doi.org/10.1007/s00442-014-2993-8, 2014.

Crosman, E. T., and Horel, J. D.: MODIS-derived surface temperature of the Great Salt Lake, Remote Sens. Environ., 113, 73-81, https://dx.doi.org/10.1016/j.rse.2008.08.013, 2009.

Gu, H., Jin, J., Wu, Y., Ek, M. B., and Subin, Z. M.: Calibration and validation of lake surface temperature simulations with the coupled WRF-lake model, Clim. Change, 129, 471-483, https://dx.doi.org/10.1007/s10584-013-0978-y, 2013.

Hakanson, L.: Models to predict Secchi depth in small glacial lakes, Aquat Sci, 57, 31-53, https://doi.org/10.1007/BF00878025, 1995.

Hostetler, S. W., and Bartlein, P. J.: Simulation of lake evaporation with application to modeling lake level variations of Harney-Malheur Lake, Oregon, Water Resour. Res., 26, 2603-2612, https://dx.doi.org/10.1029/WR026i010p02603, 1990.

Hutchinson, G. E.: A treatise on Limnology, vol. 1, Geography, Physics, and Chemsitry, John Weiley, New York, 1957.

Large, W. G., Mcwilliams, J. C., and Doney, S. C.: Oceanic vertical mixing: A review and a model with a nonlocal boundary layer parameterization, Rev. Geophys., 32, 363-403, https://dx.doi.org/10.1029/94RG01872, 1994.

Large, W. G. and Pond, S.: Sensible and latent heat flux measurements over the ocean, J. Phys. Oceanogr., 12, 464-482, https://doi.org/10.1175/1520-0485(1982)012<0464:SALHFM>2.0.CO;2, 1982.

Lei, Y., Yao, T., Bird, B. W., Yang, K., Zhai, J., and Sheng, Y.: Coherent lake growth on the central Tibetan Plateau since the 1970s: Characterization and attribution, J. Hydrol., 483, 61-67, https://dx.doi.org/10.1016/j.jhydrol.2013.01.003, 2013.

O'Brien, W. J., Barfield, M., Bettez, N., Hershey, A.E., Hobbie, J.E., Kipphut, G., Kling, G., Miller, M.C.: Long-term response and recovery to nutrient addition of a partitioned arctic lake, Freshwater. Biol., 50, 731-741, https://doi.org/10.1111/j.1365-2427.2005.01354.x, 2005.

Ping, C. L., Bockheim, J. G., Kimble, J. M., Michaelson, G. J., and Walker, D. A: Characteristics of cryogenic soils along a latitudinal transect in arctic Alaska, J. Geophys. Res., 103, 28917-28928, https://dx.doi.org/10.1029/98JD02024, 1998.

Schneider, P., Hook, S. J., Radocinski, R. G., Corlett, G. K., Hulley, G. C., Schladow, S. G., and Steissberg, T. E.: Satellite observations indicate rapid warming trend for lakes in California and Nevada, Geophys. Res. Lett., 36, L22402, https://dx.doi.org/10.1029/2009GL040846, 2009.

Wang, J., Zhu, L., Daut, G., Ju, J., Lin, X., Wang, Y., and Zhen, X.: Investigation of bathymetry and water quality of Lake Nam Co, the largest lake on the central Tibetan Plateau, China, Limnology, 10, 149-158, https://dx.doi.org/10.1007/s10201-009-0266-8, 2009.

Wetzel, R., and Likens, G. E.: Limnological Analyses, Springer, New York, 1991.

Zhang, G., Yao, T., Xie, H., Qin, J., Ye, Q., Dai, Y., and Guo, R.: Estimating surface temperature changes of lakes in the Tibetan Plateau using MODIS LST data, 119, 8552-8567, https://dx.doi.org/10.1002/2014JD021615, 2014.

Zhu, L., Xie, M., and Wu, Y.: Quantitative analysis of lake area variations and the influence factors from 1971 to 2004 in the Nam Co basin of the Tibetan Plateau, Chin. Sci. Bull., 55, 1294-1303, https://dx.doi.org/10.1007/s11434-010-0015-8, 2010.

Improving lake mixing process simulations in the Community Land Model by using K profile parameterization

Qunhui Zhang[1], Jiming Jin[1,2], Xiaochun Wang[3], Phaedra Budy[4,2], Nick Barrett[2], Sarah E. Null[2]

[1]College of Water Resources and Architectural Engineering, Northwest A & F University, Yangling, Shaanxi 712100, China

[2]Department of Watershed Sciences, Utah State University, Logan, Utah 84322, USA

[3]JIFRESSE, University of California, Los Angeles, 90095, USA

[4]US Geological Survey, Utah Cooperative Fish & Wildlife Research Unit, Logan, Utah 84322, USA

Correspondence to: Jiming Jin (jiming.jin@usu.edu)

Abstract. We improved lake mixing process simulations by applying a vertical mixing scheme, K profile parameterization (KPP), in the Community Land Model (CLM) version 4.5, developed by the National Center for Atmospheric Research. Vertical mixing of the lake water column can significantly affect heat transfer and vertical temperature profiles. However, the current vertical mixing scheme in CLM requires an ~~assumes that mixing is~~ arbitrarily enlarged eddy diffusivity ~~for~~to enhanc~~ing~~e water mixing~~driven primarily by wind, and it mostly still produces large biases in thermal process simulations~~. The coupled CLM-KPP considers a boundary layer for eddy development, and in the ~~We improved the CLM lake model by using KPP, where vertical mixing is separately for the lake boundary layer and~~ lake interior, ~~and the~~ water mixing is associated with internal wave activit~~ies~~y and shear instability~~was considers a boundary layer for eddy development~~. ~~driven by winds and surface thermal forcing, the latter representing the net heat flux in the lake boundary layer.~~ We chose ~~an~~ a lake in Arctic Alaska~~n~~ ~~lake~~ and a lake on the Tibetan Plateau to evaluate this improved lake model. Results demonstrated that CLM-KPP ~~could~~ reproduced the observed lake mixing and significantly improved lake temperature simulations when compared to the original ~~mixing scheme in~~ CLM. Our newly improved model better represents the transition between stratification and turnover~~ due to surface thermal forcing combined with high winds~~. This improved lake model has great potential for reliable physical lake process predictions and better ecosystem services.

1 Introduction

Lake thermal processes are vital to improving our understanding of regional climate systems. Lakes significantly affect regional temperature, precipitation, and surface heat fluxes (Jeffries et al., 1999; Lofgren, 2004; Long et al., 2007; Rouse et al., 2008; Thiery et al., 2015). In fact, lakes can reduce diurnal temperature variation by cooling near-surface air temperature during the day and warming it at night (Bonan, 1995; Krinner, 2003; Samuelsson et al., 2010). Regional climate modeling has shown that lakes can have a strong effect on seasonal precipitation (Diallo et al., 2017; Zhu et al., 2017). For instance, lakes cool the lower atmosphere during the summer and increase its stability, reducing summer precipitation as compared to the land (Gu et al., 2016; Sun et al., 2015). Additionally, large lakes, like the Great Lakes in North America, often produce strong snowstorms during early winter or spring from high surface evaporation (Dai et al., 2018; Laird et al., 2009). Furthermore, Rouse et al. (2005) indicated that lakes affect surface energy balance, with higher net radiation, subsurface heat storage, and evaporation than the nearby land.

Lake temperatures shape lake ecosystems (Marshall et al., 2013; Michalski and Lemmin, 1995). For example, Berger et al. (2006) showed that plankton biomass is negatively correlated with lake mixed layer depth. Some studies have proven that strong temperature stratification stimulates the spring phytoplankton bloom (Chiswell, 2011; Mahadevan et al., 2012). What is more, the frequency and intensity of water turnover, a product of the thermal processes within a lake, is critical for replenishing and circulating hypolimnetic O_2 and nutrients (Dodson, 2004; Foley et al., 2012; Shimoda et al., 2011). Stratification plays an important role in lake production and food webs. Stratification and warmer epilimnion temperatures create conditions necessary for phytoplankton production. Also, when Arctic lakes become strongly stratified, the hypolimnion can become anoxic, which in turn increases nutrient recycling and leads to elevated production the following spring (O'Brien et al., 2005). Increased food availability and warmer lake temperatures in the epilimnion from stratification increase arctic char growth. Finally, simulations of stratification date and epilimnion temperature are used in bioenergetic models to estimate fish growth and consumption and better understand Arctic char production with global environmental change (Budy and Luecke, 2014). Hence, it is important to accurately quantify lake thermal processes in order to fully comprehend how temperatures affect lake ecosystems.

Numerical models are important tools for investigating lake thermal processes. Vertical mixing processes need to be parameterized in these models. The usefulness of these models depends on whether they can represent lake processes accurately and in a dynamic consistent manner. Several one-dimensional (1-D) lake models have been developed over the last three decades with varying levels of sophistication in terms of how model physics and structure are represented (Henderson-Sellers, 1985; Hostetler and Bartlein, 1990; –Goudsmit et al., 2002; Mironov, 2008; Stepanenko et al., 2016). The Lake Model Inter-comparison Project (LakeMIP) assessed the simulation skill of different models (Stepanenko et al., 2010) and concluded that no single lake model is capable of simulating thermal processes for a wide range of lakes with different depths (Kheyrollah Pour et al., 2012; Stepanenko et al., 2014; Martynov et al., 2010; Perroud et al., 2009; Yao et al., 2014). Stepanenko et al. (2012) indicated that the poor skill in modeling lake thermal processes was due to the simplification of water mixing processes. Perroud et al. (2009) showed that insufficient water mixing weakened heat transfer within the lake, resulting in unrealistic temperature profile simulations. ~~Stepanenko et al. (2012) indicated that the poor skill in modeling lake thermal processes was due to the simplification of water mixing processes so that they were driven primarily by near-surface wind. Martynov et al. (2010) showed that focusing on wind-driven mixing often leads to insufficient water mixing and thus weakened heat transfer within the lake, resulting in unrealistic spring warming and fall cooling of the lake~~

surface . Hence, efforts have been made to improve lake mixing simulations through enlarged eddy diffusivity (Gu et al., 2013; Perroud et al., 2009; Xu et al., 2016). However, such an approach mostly strengthens mixing in the entire water body, which often greatly overestimates water mixing in the lower part of lakes (Subin et al., 2012; Zhang et al., 2018).

Based on observational studies, surface thermal forcing plays a vital role in driving lake mixing in addition to wind (MacIntyre et al., 2009). Lake water mixing is affected by not only winds, but air-lake heat exchange and net radiation as well (Chowdhury et al., 2015; Ellis et al., 1991; Imberger, 1985; Lewis, 1973; MacIntyre, 2008; Patterson et al., 1984; Yang et al., 2015). Surface thermal forcing, also called buoyancy flux, is defined as the net heat flux in the boundary layer. A lake gains energy with a positive buoyancy flux and loses energy with a negative buoyancy flux. Studies have shown that negative buoyancy fluxes combined with high winds can break up summer lake stratification (Augusto-Silva et al., 2019; Liu et al., 2019; Saber et al., 2018). Therefore, besides winds, surface thermal forcing (buoyancy flux) is an essential factor that affects lake water mixing.

K profile parameterization (KPP) (Large et al., 1994), an advanced water mixing scheme used mostly in ocean models, makes significantly improvements in oceanic water mixing simulations (Li et al., 2001; Roekel et al., 2018; Shchepetkin and McWilliamsMcwilliams, 2005; Wang et al., 2013). In KPP, eddy diffusivity is estimated separately for the lake boundary layer and lake interior. It considers a boundary layer for eddy development, and explicit inclusion of an arbitrarily enlargingeed eddy diffusivity parameter is avoided. KPP considers the effects of both wind and surface thermal forcing on water mixing. The objective of this study was is to improve lake mixing process simulations by using KPP with the Community Land Model (CLM) version 4.5, developed by the National Center for Atmospheric Research (Oleson et al., 2013). This newly improved model was then applied to an Arctic Alaskan lake and a lake called Nam Co in the Tibetan Plateau (TP) for –model validationverification. In this paper, Sect. 2 introduces the mixing schemes, data, and methodology, Sect. 3 presents simulation results and analysis, and conclusions and discussion are given in Sect. 4.

2 Mixing schemes, data, and methodology

2.1 Mixing scheme descriptions

2.1.1 The original mixing scheme in the CLM lake model

The 1-D lake model embedded in the current CLM version (CLM-ORG) simulates heat and water exchanges between the air and lake surface, water phase changes, and radiation transfer and water mixing within the lake. The lake model consists of up to 5 snow layers on the lake ice, 10 water and ice layers, 10 soil layers, and 5 bedrock layers. Researchers have attempted to advance this lake model to more closely reflect reality over the last two decades (Fang and Stefan, 1996; Henderson-Sellers, 1985; Hostetler and Bartlein, 1990; Subin et al., 2012) Mixing processes in CLM-ORG contain wind-driven eddy diffusion, an enhanced diffusion, molecular diffusion, and convective mixing. The convectionve adjustment scheme worksis activated when there is an unstably stratified water column ~~density instability~~ (Hostetler and Bartlein, 1990). The first three diffusion terms are included in the water diffusivity parameterization. T~~. T~~he total ~~eddy~~ diffusivity in the lake model is calculated as follows (Subin et al., 2012):

$$K_w^{ORG} = m_d(\kappa_e + K_{ed} + \kappa_m) \quad (1)$$

where κ_e ~~κ_e~~ represents wind-driven diffusivity (m^2 s^{-1}), K_{ed} ~~K_{ed}~~ is the enhanced eddy diffusivity ~~for unresolved~~to strengthen mixing processes (m^2 s^{-1}), κ_m ~~κ_m~~ is a constant molecular diffusivity equal to 1.4×10^{-7} m^2 s^{-1}, and m_d ~~m_d~~ is a parameter to increase the diffusivity for deep lakes, which is equal to 10 when lake depth is greater than 25 m. Wind-driven diffusivity, κ_e ~~κ_e, ,~~ is formulated as follows:

$$\kappa_e = \begin{cases} \dfrac{\kappa w^* z}{P_0(1+37R_i^2)}\exp(-k^* z), & T_g > T_f \\ 0, & T_g \le T_f \end{cases} \quad (2)$$

where T_g ~~T_g~~ is the water surface temperature (WST) (K~~),~~); T_f ~~T_f~~ is the freezing temperature, equal to 273.15 K~~,~~; κ ~~κ~~ is the von Karman constant~~,~~; P_0 ~~P_0~~ is the turbulent Prandtl number, equal to 1~~,~~; and z ~~z~~ is depth, which increases downward (m)~~.;~~ w^* ~~w^*~~ is the surface friction velocity (m s^{-1}) calculated as:

$$w^* = C_d u_2 \quad (3)$$

~~equal to 0.0012u_2,~~ where u_2 ~~u_2~~ is the 2 m wind speed (m s^{-1}~~),~~), and C_d is the drag coefficient equal to 0.0012. ~~and~~ k^* ~~k^*~~ is related to latitude φ ~~φ~~:

$$k^* = 6.6 u_2^{-1.84}\sqrt{|sin\varphi|} \quad (~~3~~4)$$

~~$k^* = 6.6 u_2^{-1.84}\sqrt{|\sin\varphi|}$~~

R_i ~~R_i~~ is the Richardson number, given as:

$$R_i = \frac{-1+\sqrt{1+\dfrac{40N^2\kappa^2 z^2}{w^{*2}\exp(-2k^* z)}}}{20} \quad (~~4~~5)$$

where N ~~N~~ is the local buoyancy frequency representing the stability of water (s^{-1}),

$$N^2 = \frac{g}{\rho}\frac{\partial\rho}{\partial z} \quad (~~5~~6)$$

g ~~g~~ is gravity acceleration (m s^{-2}), and ρ ~~ρ~~ is the density of water (kg m^{-3}). The equation of the enhanced diffusivity is:

~~$K_{ed} = 1.04\times10^{-8}(N^2)^{-0.43}, (N^2 \ge 7.5\times10^{-5}\ s^2)$ (6)~~

$$K_{ed} = 1.04\times10^{-8}(N^2)^{-0.43}, (N^2 \ge 7.5\times10^{-5}\ s^{-2}) \quad (7)$$

When N^2 ~~N^2~~ ~~is the minimum reaching to about~~reached at least 7.5×10^{-5} s^{-2}~~2~~, the enhanced diffusivity is about six times ~~more~~ greater than the molecular diffusivity (Fang and Stefan, 1996). The wind-driven diffusivity is typically at least 2 orders larger than the molecular diffusivity (Hostetler and Bartlein, 1990). Thus, winds have a dominant effect on water mixing in the CLM lake model. In practical application, the total ~~eddy~~ diffusivity computed by Eq. (1) generally produces unrealistically weak mixing and causes large errors in temperature profile simulations (Gu et al., 2013; Zhang et al., 2018).

2.1.2 KPP

KPP has two different ~~eddy~~ diffusivity parameterizations for the lake boundary layer and the layer below, which is different from the ~~eddy~~total diffusivity represented in the original CLM lake model. The diffusivity of the lake boundary layer, a function of ~~wind and~~ surface ~~thermal~~ forcing and the lake boundary layer depth, is based on the Monin-~~-~~Obukhov similarity theory (Monin and Obukhov, 1954):

$$K_w^{KPP}(\sigma) = hw(\sigma)G(\sigma) + \kappa_m \quad (~~7~~8)$$

~~Where~~where $\sigma = d/h$ ~~$\sigma = d/h$~~ is the dimensionless vertical coordinate varying from 0 at the lake surface to 1 at the bottom of the lake boundary layer h ~~(h)~~, $w(\sigma)$ ~~$w(\sigma)$~~ is the velocity scale, and $G(\sigma)$ ~~$G(\sigma)$~~ is the shape function. κ_m ~~κ_m~~ is a constant molecular diffusivity (m^2 s^{-1}), as in Eq. (1). The velocity scale is:

$$w(\sigma) = \begin{cases} \dfrac{\kappa u^*}{\emptyset\left(\dfrac{\varepsilon h}{L}\right)}, \varepsilon < \sigma < 1, \zeta < 0 \\ \dfrac{\kappa u^*}{\emptyset\left(\dfrac{\sigma h}{L}\right)}, \quad otherwise \end{cases} \quad (~~8~~9)$$

where κ ~~κ~~ is the von Karman constant (0.4), ε ~~ε~~ is equal to 0.1, and u^* ~~u^*~~ is the surface friction velocity (m s^{-1}) calculated as (Large and Pond, 1982):

$$u^{*2} = \frac{\rho_a}{\rho} C_d U^2 \quad (10)$$

$$10^3 C_d = \frac{2.70}{U} + 0.142 + 0.0764U \quad (11)$$

where ρ_a and ρ are the air and lake water densities (kg m^{-3}), respectively, C_d is the drag coefficient, and U is the 10 m wind speed (m s^{-1}). $\emptyset(\zeta)$ is a non-dimensional flux profile associated with the stability parameter $\zeta = d/L = \sigma h/L$, and L is the Monin-Obukhov length scale defined as:

$$L = u^{*3}/\kappa B_f \quad (12)$$

where B_f is the buoyancy flux (m^2 s^{-3}):

$$B_f = H^* g\alpha C_p{}^{-1}\rho^{-1} \quad (13)$$

H^* is the sum of the surface turbulent heat fluxes, net long-wave radiation, and net shortwave radiation for the lake boundary layer (W m^{-2}), α is the constant thermal expansion coefficient, and C_p is the specific heat capacity of water (J kg^{-1} K^{-1}). The non-dimensional shape function $G(\sigma)$ is a third-order polynomial (see the Appendix).

~~, $\phi(\zeta)$ is a non-dimensional flux profile associated with the stability parameter $\zeta = d/L = \sigma h/L$, L is the Monin-Obukhov length scale defined as $L = u^{*3}/\kappa B_f$, and the buoyancy flux $B_f = H^* g\alpha C_p^{-1}\rho^{-1}$. H^* is the sum of the surface turbulent heat fluxes, net long-wave radiation, and net shortwave radiation for the lake boundary layer, α is the constant thermal expansion coefficient, and C_p is the specific heat capacity of water (J kg^{-1} K^{-1}). The non-dimensional shape function $G(\sigma)$ is a~~

~~third-order polynomial (see the Appendix).~~

Water mixing below the lake boundary layer considers vertical shear and internal waves. The equation is:

$$K_w^{KPP} = k_s + k_w + \kappa_m$$ (~~9~~14)

where k_s ~~k_s~~ is the diffusivity due to shear instability (m² s⁻¹), and k_w ~~k_w~~ is the internal wave diffusivity set to a constant (10^{-7} m^2 s^{-1}) as the background diffusivity (Bryson and Ragotzkie, 1960; Powell and Jassby, 1974; Thorpe and Jiang, 1998). The shear mixing term is calculated as:

$$k_s = \begin{cases} k_0, & Ri_g < 0 \\ k_0\left[1-(Ri_g/Ri_0)^2\right]^{p}, & 0 < Ri_g < Ri_0 \\ 0, & Ri_0 < Ri_g \end{cases}$$ (~~10~~15)

where k_0 ~~k_0~~ = 10^{-5} m^2 s^{-1} (Etemad-Shahidi and Imberger, 2006; ~~Saber et al., 2018;~~ Sweers, 1970), Ri_0 ~~Ri_0~~ = 0.7 , and p ~~p~~ = 3. Ri_g ~~Ri_g~~ is the local gradient Richardson number:

$$Ri_g = \frac{N^2}{\left(\frac{\partial V}{\partial z}\right)^2}$$ (~~11~~16)

$$V = V_{sfc}(3\left(\frac{z}{D}\right)^2 - 4\left(\frac{z}{D}\right) + 1)$$ (~~12~~17)

$$V_{sfc} = 0.028W$$ (~~13~~18)

where V ~~V~~ is the horizontal velocity of water (m ~~/~~s⁻¹), D ~~D~~ is the lake depth (m), V_{sfc} ~~V_{sfc}~~ is the surface water flow velocity (m s⁻¹), and W ~~W~~ is the surface wind (m s⁻¹). To apply KPP in the CLM lake model, we use Eq. (~~12~~17) to represent the change of water flow in the vertical direction over the entire lake depth ~~(~~D ~~D)~~ (Banks, 1975; ~~Jan and~~ Verhagen, 1994). We can see in Eq. (~~13~~18) that V_{sfc} ~~V_{sfc}~~ is linked with W ~~W~~ (Stanichny et al., 2016; Wu, 1975).

The boundary layer depth depends mainly on the buoyancy and horizontal water flow velocity profiles. In order to compute the boundary layer depth, the bulk Richardson number is first computed as follows:

$$Ri_b(d) = \frac{\left(B_r - B(d)\right)d}{|V_r - V(d)|^2 + V_t^2(d)}$$ (~~14~~19)

where Ri_b ~~Ri_b~~ is the bulk Richardson number, and B ~~B~~ is the buoyancy. When Ri_b ~~Ri_b~~ is equal to 0.25 (Kunze et al., 1990; Peters et al., 1995), the shallowest water depth (d) ~~(d)~~ is treated as the depth of the lake boundary layer. The subscript r ~~r~~ represents the near-surface water layer with a depth of 0.1 m ($B_r, B(d), V_t^2(d)$, see the Appendix).

In this study, KPP was implemented into the CLM lake model (CLM-KPP) to improve lake mixing process simulations. ~~The difference of the current mixing parameterization of the CLM (CLM-ORG) and the KPP (CLM-KPP) is in the equations used to estimate eddy diffusivity. I~~In ~~CLM-~~KPP~~,~~, eddy diffusivity is estimated separately for the lake boundary layer and lake interior. In the lake boundary layer, the eddy diffusivity is determined not by the local gradient of mean variables, but by surface forcing and the boundary layer depth. The non-local effect is taken into account by estimating the boundary layer depth first, and eddy diffusivity is then specified with a prescribed profile in the lake boundary layer. In the lake interior, mixing is ~~generally weak and~~ associated with internal wave activit~~y~~iesy and shear instability. However, ~~The major~~

~~shortcomings of the original eddy diffusion scheme in~~ CLM-ORG ~~are that it~~ does not consider a boundary layer for eddy development~~,~~, and ~~and~~ insufficient water mixing is enhanced through ~~it requires~~ an ad hoc parameter, which is often unable to reflect ~~the~~ reality (Zhang et al., 2018). Thus, the coupling of CLM-KPP is essential ~~to~~for better understanding of lake mixing processes. ~~to enhance the estimated eddy diffusivity.~~

~~In the KPP scheme, an explicit inclusion of an ad hoc enlarging parameter is avoided.~~

~~**In this study, KPP was implemented into the CLM lake model (CLM-KPP) to improve lake mixing process simulations. As with CLM-ORG, the input variables to KPP consist of the lake depth, surface wind, and water density of each layer. In addition, KPP needs the buoyancy flux for the lake boundary layer. Outputs from KPP contain the total eddy diffusivity of each layer and the lake boundary layer depth.**~~

2.2 Study area

We selected two lakes with available data ~~an Arctic Alaskan lake with available data~~ to evaluate the original lake mixing scheme and KPP. Fog~~-~~3 Lake is in Arctic Alaska at (68.67˚ N, 149.10˚ W) (Fig. 1a). In 2018 it had a surface area of ~~35~~38,~~230~~ 863 m^2 and a maximum depth of ~~19.74~~21 m. The lake has a long ice duration, and ice-off is usually in late June, while ice-on typically occurs in early October (Arp et al., 2015). Around this lake, the mean annual air temperature is about ~ –6 ℃, and the mean annual precipitation is ~ 200 mm (Ping et al., 1998). This kettle lake is surrounded by lower hills covered mainly with shrubs and tundra. Due to the treeless landscape, there are no shielding effects on the wind. In addition, Fog3 Lake is formed by glaciers, and has less connection to other surrounding surface waters.

The second lake is Nam Co, the highest and largest lake in the central TP (Fig. 1b). It is situated over 30.5–30.95˚ N, 90.2–91.05˚ E with an altitude of 4,730 m and a surface area of about 2,021 km^2 in 2010 (Lei et al., 2013; Zhu et al., 2010). Its maximum depth reaches more than 95 m, and the mean depth is about 40 m (Wang et al., 2009). The main water supply to Nam Co is precipitation and melting glaciers. Nam Co is a closed lake with no outflow, and water loss occurs mainly through evaporation (Ma et al., 2016).

2.3 Data

Observed hourly meteorological station data for Fog3 Lake were used to ~~force~~ drive CLM ~~with the two water mixing schemes: the wind-only driven scheme~~-ORG and CLM-KPP. Fog3 Lake is about 1.5 km from Toolik Field Station (68°37.796' N, 149°35.834' W), in the northern foothills of the Brooks Mountain Range, Alaska (https://toolik.alaska.edu/edc/abiotic_monitoring/index.php). ~~The weather station is on the shore of Fog3 Lake, and Utah State University runs the measurements included in this study.~~ ~~This station is ~1.5 km from Fog 3 Lake, and t~~The forcing variables include downward shortwave and longwave radiation, wind speed, air temperature, air pressure, and specific humidity. Observed lake temperatures from 1 July through 31 August 2018 are for lake depths of 0, 1, 2, 3, 4, 5, 6, 7, 8, 10, 12, 14, and 16 m for model initialization and evaluation.

For Nam Co, the forcing data were from the gridded China meteorological dataset developed by the hydro-meteorological research group at the Institute of Tibetan Plateau Research, Chinese Academy of Sciences (ITPCAS) (Chen et al., 2011; He and Yang, 2011). The forcing variables in this dataset are the same as those for the Alaskan lake. The ITPCAS data cover the period 1979–2015 with a spatial resolution of 0.1 degree and a time step of 3 h. We used the Nam Co meteorological station data for the period of October 2005 through December 2010 to assess the ITPCAS forcing variables. These forcing variables agreed very well with the Nam Co station data, except the wind speed showed significant biases (Figs. not shown). Linear regression with the station wind speed was applied to correct these biases. Monthly Moderate Resolution Imaging Spectroradiometer (MODIS) surface temperature data at a spatial resolution of 0.05 degree (Savtchenko et al., 2004; Wan et al., 2010) were applied to evaluate the model results for Nam Co. Previous studies have ~~evaluat~~verified MODIS ~~water surface temperature~~WST data for lakes ~~based on~~with *in situ* observations (Crosman and Horel, 2009; Schneider et al., 2009). Zhang et al. (2014) ~~compar~~founed that the nighttime ~~water surface temperature~~WST of MODIS for Nam Co ha~~s~~d a 0.89 correlation coefficient and a –1.4 ℃ bias when compared with surface observations.~~and *in situ* observations for Nam Co with a correlation coefficient of 0.89 and a bias of -1.4 ℃~~ All these studies show~~ed~~ that the MODIS WST has ~~an~~ acceptable accuracy for studying lake thermal processes.~~, which showed an acceptable accuracy for MODIS. Thus, due to limited observed temperature data for Nam Co, we chose MODIS data to validate CLM-ORG and CLM-KPP.~~

2.4 Experiment design

Simulations for Fog3 Lake were conducted with both CLM-ORG and CLM-KPP from 1 July through 31 August 2018. The depth for this lake was set ~~up to~~at 20 m in both models. We divided the lake into 24 layers, with layer center point depths of 0.05, 0.15, 0.25, 0.35, 0.45, 1, 2, 3, 4, 5, 6, 7, 8, 9, 10, 11, 12, 13, 14, 15, 16, 17, 18, and 19.25 m. Observed lake temperatures for Fog3 Lake are for lake depths of 0, 1, 2, 3, 4, 5, 6, 7, 8, 10, 12, 14, and 16 m. The lake model has 10 lake layers by default, and the center point depths of these layers are 0.05, 0.3, 0.9, 1.9, 3.3, 5.1, 7.5, 10.3, 13.79, and 17.94 m generated automatically by the layering scheme in the model based on the input lake depth. For this study, we tried to keep each layer thin in the top part of the lake to reflect diurnal cycles (layers 1–5) in both CLM-ORG and CLM-KPP. Below layer 5, we used mostly the observed points to layer the rest of the lake column. Finally, we produced 24 layers for the entire lake column in both models, and the center point depths of these lake layers are 0.05, 0.15, 0.25, 0.35, 0.45, 1, 2, 3, 4, 5, 6, 7, 8, 9, 10, 11, 12, 13, 14, 15, 16, 17, 18, and 19.25 m, respectively. ~~The simulations of CLM-ORG with both 10 and 24 layers were very similar (Figs. not shown), while the simulations of CLM-KPP with 24 layers were closer to observations than those with 10 layers when the water mixing event occurred. These results indicated that a high resolution layering in CLM-KPP may be important for simulating lake water mixing. We divided the lake into 24 layers, with layer center point depths of 0.05, 0.15, 0.25, 0.35, 0.45, 1, 2, 3, 4, 5, 6, 7, 8, 9, 10, 11, 12, 13, 14, 15, 16, 17, 18, and 19.25 m.~~ The lake temperatures were initialized with observations for 1 July 2018. The WST and temperature profile simulations with

CLM-ORG and CLM-KPP were compared with the observed lake temperatures. For Nam Co, we ~~still~~also used 10 default layers for lake depths in our models without observed vertical temperature profiles, and ~~the~~ lake depths were set based on observations (Wang et al., 2009), which ranged from 20 to 95 m. There were 34 model grid cells covering Nam Co with a spatial resolution of 0.1 degree.

~~The data for Nam Co were used mainly for model validation. The lake depths of the total 34 grid cells simulated for Nam Co ranged from 20 to 95 m (Wang et al., 2009). Each water column was divided same as the CLM lake default vertical discretization. The default 50 m lake water body was divided into 10 layers with each layer thickness of 0.1, 1, 1, 2, 3, 4, 5, 7, 7, 10.45, 10.45 m. The top layer thickness was kept to 0.1 m and the other layer (except for the bottom layer) was adjusted using the proportions compared to the lake depth of 50 m.~~ The temperature of each layer was initialized with 277 K. The simulated period for Nam Co was from 2001 through 2012. The simulations for the first two years were discarded as model spin-up, and the remaining simulations were used for analysis. The metrics used for evaluating the performance of the model included the root mean square error (RMSE) and correlation coefficient (R).

3 Results

3.1 Simulations for Fog3 Lake with CLM-ORG and CLM-KPP

WST simulations with CLM-KPP were more accurate than those with CLM-ORG, especially in August. The RMSE of WST decreased from 0.8 ˚C with CLM-ORG to 0.4 ˚C with CLM-KPP (Fig. 2). CLM-KPP also produced better vertical lake temperature profile simulations than CLM-ORG, particularly in mid to late August. The observations showed that the lake mixed on 16 August (Fig. 3a). CLM-KPP accurately captured the mixing event (Fig. 3c), while CLM-ORG ~~estimated a stratified lake~~produced strong stratification in the upper part of the lake throughout the ~~model~~ simulation period (Fig. 3b). Insignificant differences were seen between CLM-ORG and CLM-KPP when compared to observations for the period before 16 August (Table 1), while remarkable improvements were achieved with CLM-KPP during 16–31 August after ~~the~~ a strong wind event occurred (Figs. 3d~~–~~–e). The RMSE of the temperature profile simulations decreased from 1.~~2~~4 ˚C with CLM-ORG to ~~1~~0.3~~0~~ ˚C with CLM-KPP, and R increased from 0.~~90~~57 to 0.9~~5~~9 ~~during~~for 16–31 August 2018 (Table 1). In general, CLM-KPP had superior performance in simulating well-mixed conditions when compared with CLM-ORG, indicating a successful implementation of KPP into CLM.

Simulations of total diffusivity (m^2~~/~~ s^{-1}) K_w^{KPP} with CLM-KPP were compared with those of K_w^{ORG} with CLM-ORG. K_w^{KPP} within the boundary layer was generally larger than K_w^{ORG}, especially in August (Fig. 4). ~~Thermal forcing played a vital role in this enlarged diffusivity, which was considered only in CLM-KPP and not in CLM-ORG.~~ However, the total diffusivity with CLM-ORG was higher than that with CLM-KPP below the boundary layer (Fig. 4). The pattern of the diffusivity with CLM-ORG was consistent with that of the squared buoyancy frequency N^2~~N^2~~ (Fig. 5), implying that the enhanced diffusivity ($K_{ed}$$K_{ed}$) was weighted very highly in K_w^{ORG} in this model. In the meantime, K_w^{KPP} was mostly on the order of 10^{-7} m^2 s^{-1} and was the product sum of internal-wave diffusivity, molecular diffusivity, and diffusivity due to shear instability (Eq. (914)). The first two terms were also on the order of 10^{-7} m^2 s^{-1}, indicating that the total diffusivity with CLM-KPP was controlled mostly by these two terms. In early July, K_w^{KPP} sometimes appeared to be on the order of 10^{-5} m^2 s^{-1}, which was consistent with that of the last term, shear instability diffusivity, implying that this term dominated K_w^{KPP}. The diffusivity increase was closely related to the strong winds occurring at the same time (Fig. 4b).

The squared buoyancy frequency ($N^2$$N^2$) of simulations with both CLM-KPP and CLM-ORG were also compared for our study period. $N^2$$N^2$ was related to the water density gradient (Eq. (56)) determined by the temperature gradient in both models. A greater $N^2$$N^2$ produced more stable water and stronger water stratification. From 1 July through 15 August, the simulated $N^2$$N^2$ with CLM-KPP near the bottom of the boundary layer was slightly larger than that with CLM-ORG (Fig. 5). Thus, the simulated water stratification with CLM-KPP at the bottom of the boundary layer was stronger than that in CLM-ORG before 16 August. However, after 16 August, the maximum $N^2$$N^2$ with CLM-ORG occurred in the middle layer of the lake, maintaining stratification there. Conversely, the maximum $N^2$$N^2$ with CLM-KPP moved down to near the bottom of the lake during the same 16-day period (Fig. 5).

3.2 Analysis of CLM-KPP simulations for Fog3 Lake

We examined our simulations and meteorological forcing data in detail to physically understand water mixing conditions simulated by CLM-KPP, especially over the period of 16–31 August 2018. Figure 6a shows that downward shortwave radiation was 45 W m^{-2} less during 1–15 August (shaded area) than in July. Meanwhile, over the same period, air temperature and specific humidity decreased dramatically, while wind speed showed almost no trend (Figs. 6b––d). In this period, the simulated net radiation with CLM-KPP was 54 W m^{-2} lower than that for July (Fig. 6e). The turbulent heat flux, the sum of sensible and latent heat fluxes, increased over this 15-day period due mainly to the decreased air temperature and humidity (Fig. 6f). Figure 6g shows that buoyancy flux, defined as net radiation minus turbulent heat flux in the boundary layer with a different unit (m^2 /s^{-3}), was mostly negative during 1–15 August, showing that the lake was losing heat. Due to this heat loss, the temperature in the upper lake decreased, reducing the temperature difference between the upper and lower parts of the lake and thus weakening the stratification. Therefore, we can see that the boundary layer depth increased over the period of 1–15 August (Fig. 6h) when the wind had no systematic changes, but the thermal forcing (buoyancy flux) played a significant role in this increase.

During 15–16 August, a wind event (12 m /s^{-1}) mixed the lake, dramatically increasing the boundary layer depth in addition to the negative buoyancy flux. The deep boundary layer was maintained through the end of August, even though the winds returned to normal conditions. Such strong mixing was not seen in CLM-ORG, where the water stratification could not be broken up by the high wind event without help from the negative buoyancy fluxthermal forcing. Hence, without the negative thermal forcing had a critical effect on the strong mixing in our study lake, which was consistent with observations. an ad hoc parameter to enhance the water diffusivity as in CLM-ORG, CLM-KPP still could reproduced the observed water mixing processes.

3.3 Model validation with Nam Co data

We validated both CLM-ORG and CLM-KPP with MODIS data for Nam Co by conducting 10-km spatial resolution simulations for this lake over the period of 2003 through 2012. We can see that CLM-KPP improved WST simulations averaged over the entire lake (34 model grid cells) when compared with the MODIS data and CLM-ORG simulations (Fig. 7). The RMSE of WST decreased from 4.58 ˚C with CLM-ORG to 2.23 ˚C with CLM-KPP, and R increased from 0.90 to 0.96 at the same time.

The improved WST simulations with CLM-KPP were closely related to the water diffusivity simulations with KPP as discussed above. We averaged the K_w^{ORG} and K_w^{KPP} simulations over water columns with depth greater than 25 m for Nam Co, as shown in Fig. 8, and the total of such columns were 28 out of 34 for this lake. Figure 8 indicates that K_w^{KPP} was slightly smaller than K_w^{ORG} mostly in the mixing layer of the lake over the summer. The difference likely resulted from the enlarged K_w^{ORG} in CLM where this parameter was increased by a factor of 10 when the lake depth was greater than 25 m. In the deeper part of the lake, K_w^{KPP} was much smaller than K_w^{ORG} over the summer due much to the contribution of K_{ed} to K_w^{ORG}. In the spring and fall, K_w^{KPP} was significantly larger than K_w^{ORG}. During the winter when the lake froze, both CLM-KPP and CLM-ORG were set to use K_w^{ORG}. We can see that the most significant improvements in WST for Nam Co occurred during the ice-free seasons when KPP was activated. Overall, CLM-KPP can enhance eddy diffusivity during spring and fall and maintain weak eddy diffusivity in the lake interior during summer when stratification is strong.

4 Conclusions and discussion

We improved lake mixing process simulations by applying the vertical mixing scheme KPP in CLM. The current vertical mixing scheme in CLM is driven mainly by winds, while KPP considers not only winds but surface thermal forcing as well. The improved lake model was applied to Fog 3 Lake in an Arctic Alaskan lake and to Nam Co lake in the TP for model evaluation. Results for the Alaskan lake indicate that the WST and lake temperature profile simulations using KPP are greatly improved when compared to the original vertical mixing scheme in CLM. During the transition season in August, the improvement is most obvious. This improvement is associated with negative heat flux and high wind, which can cause deepening of the boundary layer and strong mixing. However, the original vertical mixing scheme of CLM cannot capture these strong mixing events and causes a positive lake temperature bias in its simulation. CLM-KPP was further validated with the observed data from Nam Co, and results showed that WST simulations were significantly improved when compared with the MODIS data and CLM-ORG simulations.

More data are needed to further verify CLM-KPP, including atmospheric forcing data over lakes and observed lake temperature profiles. It should also be noted that although CLM-KPP has improved thermal process simulations, large WST biases still existed during the ice freezing period for Nam Co. Such biases most likely resulted from the oversimplified lake ice scheme in the CLM lake model. Therefore, a more realistic ice scheme in lake models is needed for better understanding of the effects of water mixing on ice formation. In general, this coupled model provides an important tool for lake hydrology and ecosystem studiesThe improved lake model should be useful for reliable lake process predictions and better ecosystem services..

Appendix

Lake temperature is calculated as follows:

$$\frac{\partial T}{\partial t}=\frac{\partial}{\partial z}\left\{K_w(z,t)\frac{\partial T}{\partial z}\right\}+\frac{1}{C_w}\frac{\partial \phi}{\partial z} \tag{A1}$$

where T T is lake temperature (K) at depth z z (m) and time t t (s), ϕ ϕ is the absorbed solar radiation flux as a heat source term (W m^{-2}), C_w C_w is the volumetric heat capacity of lake water (J m^{-3} K^{-1}), and K_w is the total eddy diffusivity (m^2 s^{-1}).

The non-dimensional flux profiles are calculated as follows:

$$\emptyset=\begin{cases}1+5\zeta, & 0\le\zeta\\ (1-16\zeta)^{-1/2}, & -1.0\le\zeta<0\\ (-28.86-98.96\zeta)^{-1/3}, & \zeta<-1.0\end{cases} \tag{A2}$$

The non-dimensional shape function $G(\sigma)$ $G(\sigma)$ is a third-order polynomial:

$$G(\sigma)=a_0+a_1\sigma+a_2\sigma^2+a_3\sigma^3 \tag{A3}$$

a_0, a_1, a_2, and a_3 are given as:

$$a_0=0 \tag{A4a}$$

$$a_1=1 \tag{A4b}$$

$$a_2=-2+3\frac{\upsilon(h)}{hw(1)}+\frac{\partial\upsilon(h)}{w(1)}+\frac{\upsilon(h)\partial w(1)}{hw(1)^2} \tag{A4c}$$

$$a_3=1-2\frac{\upsilon(h)}{hw(1)}-\frac{\partial\upsilon(h)}{w(1)}-\frac{\upsilon(h)\partial w(1)}{hw(1)^2} \tag{A4d}$$

where $\upsilon(h)$ $\upsilon(h)$ is the water total diffusivity as a function of lake depth (h) (h), and $w(1)$ $w(1)$ is the velocity scale at the bottom of the lake boundary layer, $\partial\upsilon(h)$ is the lake depth derivative of υ, and $\partial w(1)$ is the lake depth derivative of w at the bottom of the lake boundary layer..

$B(d)$ $B(d)$ is the buoyancy difference calculated with a depth of d d as:

$$B(d)=g\left(1-\frac{\rho_r}{\rho(d)}\right) \tag{A5}$$

V_t^2 is calculated as:

$$V_t^2(d)=\frac{C_v dNw_s(-\beta_T C_s\varepsilon)^{-1/2}}{Ri_c\kappa^2} \tag{A6}$$

where Ri_c Ri_c = 0.25, C_v C_v = 1.6, β_T β_T = 0.2, and C_s C_s = –98.96.

Code and data availability

The model configuration and the input data used in this study are available based upon request.

Author contribution

Qunhui Zhang conducted the modeling, performed the analysis, and drafted the manuscript; Jiming Jin designed the study, interpreted the results, and supervised the research; Xiaochun Wang contributed the original ideas of the research; Phaedra Budy and Nick Barrett provided observational data and helped with the study design and data analysis; Sarah ~~E.~~ Null gave constructive comments on the results ~~in this study~~. All ~~the~~ authors edited the manuscript.

Competing interests

The authors declare that they have no conflict of interest.

Acknowledgments

~~This work was supported by the National Natural Science Foundation of China [grant number 91637209] and a grant from the US National Science Foundation [grant number 1603088].~~This work was supported by the National Natural Science Foundation of China [grant numbers 91637209, 41571030, and 91737306] and a grant from the US National Science Foundation [grant number 1603088]. Q.Z. was also supported by the National Key R&D Program of China on monitoring, early warning, and prevention of major natural disasters (No. 2018YFC150703). J.J. was also supported by Utah Agricultural Experiment Station.

References

Arp, C. D., Jones, B. M., Liljedahl, A. K., Hinkel, K. M., and Welker, J. A.: Depth, ice thickness, and ice-out timing cause divergent hydrologic responses among Arctic lakes, Water Resour. Res., 51~~(12)~~, 9379–9401, https://dx.doi.org/10.1002/2015WR017362, 2015.

~~Augusto-Silva, P. B., MacIntyre, S., de Moraes Rudorff, C., Cortés, A., and Melack, J. M.: Stratification and mixing in large floodplain lakes along the lower Amazon River, J. Great Lakes Res., 45(1), 61-72. https://dx.doi.org/10.1016/j.jglr.2018.11.001, 2019.~~

Banks, R. B.: Some features of wind action in shallow lakes, Proc. Am. Soc. Civ. Eng., 101, 813–827, 1975.

Berger, S. A., Diehl, S., Kunz, T. J., Albrecht, D., Oucible, A. M., and Ritzer, S.: Light supply, plankton biomass, and seston stoichiometry in a gradient of lake mixing depths, Limnol. Oceanogr., 51~~(4)~~, 1898–1905, https://dx.doi.org/10.4319/lo.2006.51.4.1898, 2006.

Bonan, G. B.: Sensitivity of a GCM simulation to inclusion of inland water surface, J. Climate, 8~~(11)~~, 2691–2704, https://dx.doi.org/10.1175/1520-0442(1995)008%3C2691:SOAGST%3E2.0.CO;2, 1995.

Bryson, R. A., and Ragotzkie, R. A.: On internal waves in lakes, Limnol. Oceanogr., 5, 397–408, https://dx.doi.org/10.4319/lo.1960.5.4.0397, 1960.

Budy, P. and Luecke, C.: Understanding how lake populations of arctic char are structured and function with special consideration of the potential effects of climate change: A multi-faceted approach, Oecologia, 176, 81–94, https://dx.doi.org/10.1007/s00442-014-2993-8, 2014.

Bryson, R. A., and Ragotzkie, R. A.: On internal waves in lakes, Limnol. Oceanogr., 5(4), 397-408, https://dx.doi.org/10.4319/lo.1960.5.4.0397, 1960.Chen, Y., Yang, K., He, J., Qin, J., Shi, J., Du, J., and He, Q.: Improving land surface temperature modeling for dry land of China, J. Geophys. Res.-Atmos., 116, https://dx.doi.org/10.1029/2011JD015921, 2011.

Chiswell, S. M.: Annual cycles and spring blooms in phytolankton: Don't abandon Sverdrup completely, Mar. Ecol.-Prog. Ser., 443, 39-50, 2011.

Chowdhury, M. R., Wells, M. G., and Cossu, R.: Observations and environmental implications of variability in the vertical turbulent mixing in Lake Simcoe, J. Great Lakes Res., 41(4), 995-1009, https://dx.doi.org/10.1016/j.jglr.2015.07.008, 2015.Crosman, E. T., and Horel, J. D.: MODIS-derived surface temperature of the Great Salt Lake, Remote Sens. Environ., 113, 73–81, https://dx.doi.org/10.1016/j.rse.2008.08.013, 2009.

Dai, Y., Yao, T., Li, X., and Ping, F.: The impact of lake effects on the temporal and spatial distribution of precipitation in the Nam Co basin, Tibetan Plateau, Quatern. Int., 475, 63–-69, https://dx.doi.org/10.1016/j.quaint.2016.01.075, 2018.

Diallo, I., Giorgi, F., and Stordal, F.: Influence of Lake Malawi on regional climate from a double-nested regional climate model experiment, Clim. Dynam., 50(9-10), https://dx.doi.org/10.1007/s00382-017-3811-x, 2017.

Dodson, S. I.: Introduction to limnology, J. N. Am. Benthol. Soc., 23(3), 661-662, https://dx.doi.org/10.1899/0887-3593(2004)023%3C0661:ITL%3E2.0.CO;2, 2004.

Ellis, C. R., Stefan, H. G., and Gu, R.: Water temperature dynamics and heat transfer beneath the ice cover of a lake, Limnol. Oceanogr., 36(2), 324-334, https://dx.doi.org/10.4319/lo.1991.36.2.0324, 1991.

Etemad-Shahidi, A., and Imberger, J.: Diapycnal mixing in the thermocline of lakes: Estimation by different methods, Environ, Fluid Mech., 6(3), 227-240, https://dx.doi.org/10.1007/s10652-005-4480-6, 2006.

Fang, X., and Stefan, H. G.: Long-term lake water temperature and ice cover simulations/measurements, Cold Reg. Sci. Technol., 24(3), 289-304, https://dx.doi.org/10.1016/0165-232X(95)00019-8, 1996.

Foley, B., Jones, I. D., Maberly, S. C., and Rippey, B., Long-term changes in oxygen depletion in a small temperate lake: Effects of climate change and eutrophication. Freshwater Biol., 57(2), 278–-289, https://dx.doi.org/10.1111/j.1365-2427.2011.02662.x, 2012.

Goudsmit, G. H., Burchard, H., Peeters, F., and Wüest, A.: Application of k-ε turbulence models to enclosed basins: The role of internal seiches, J. Geophys. Res.-–Oceans, 107(C12), 23-1-23-133230, https://dx.doi.org/10.1029/2001JC000954, 2002.

Gu, H., Jin, J., Wu, Y., Ek, M. B., and Subin, Z. M.: Calibration and validation of lake surface temperature simulations with the coupled WRF-lake model, Clim. Change, 129(3-4), 471–483, https://dx.doi.org/10.1007/s10584-013-0978-y, 2013.

Gu, H., Ma, Z., and Li, M.: Effect of a large and very shallow lake on local summer precipitation over the Lake Taihu basin in China, J. Geophys. Res.-Atmos., 121(15), 8832–8848, https://dx.doi.org/10.1002/2015JD024098, 2016.

He, J., and Yang, K.: China Meteorological Forcing Dataset, Cold and Arid Regions Science Data Center, Lanzhou, https://dx.doi.org/10.3972/westdc.002.2014.db, 2011.

Henderson-Sellers, B.: New formulation of eddy diffusion thermocline models, Appl. Math. Model., 9(6), 441–446, https://dx.doi.org/10.1016/0307-904X(85)90110-6, 1985.

Hostetler, S. W., and Bartlein, P. J.: Simulation of lake evaporation with application to modeling lake level variations of Harney-Malheur Lake, Oregon, Water Resour. Res., 26(10), 2603–2612, https://dx.doi.org/10.1029/WR026i010p02603, 1990.

Imberger, J.: The diurnal mixed layer, Limnol. Oceanogr., 30(4), 737-770, https://dx.doi.org/10.4319/lo.1985.30.4.0737, 1985.

Jan, H. G., and Verhagen.: Modeling phytoplankton patchiness under the influence of wind-driven currents in lakes, Limnol. Oceanogr., 39(7), 1551-1565, https://dx.doi.org/10.4319/lo.1994.39.7.1551, 1994.

Jeffries, M. O., Zhang, T., Frey, K., and Kozlenko, N.: Estimating late-winter heat flow to the atmoshere from the lake-dominated Alaskan north slope, J. Glaciol., 45(150), 315–324, https://dx.doi.org/10.3189/S0022143000001817, 1999.

Kheyrollah Pour, H., Duguay, C. R., Martynov, A., and Brown, L. C.: Simulation of surface temperature and ice cover of large northern lakes with 1-D models: A comparison with MODIS satellite data and in situ measurements, Tellus A, 64(1), 17614, https://dx.doi.org/10.3402/tellusa.v64i0.17614, 2012.

Krinner, G.: Impact of lakes and wetlands on boreal climate, J. Geophys. Res., 108(D16), 4520, https://dx.doi.org/10.1029/2002JD002597, 2003.

Kunze, E., Williams, A. J., and Briscoe, M. G.: Observations of shear and stability from a neutrally buoyant float, J. Geophys. Res., 95(C10), 18127–18142, https://dx.doi.org/10.1029/JC095iC10p18127, 1990.

Laird, N. F., Desrochers, J., and Payer, M.: Climatology of lake-effect precipitation events over Lake Champlain, J. Appl. Meteorol. Clim., 48(2), 232–250, https://dx.doi.org/10.1175/2008JAMC1923.1, 2009.

Large, W. G., MewilliamsMcWilliams, J. C., and Doney, S. C.: Oceanic vertical mixing: A review and a model with a nonlocal boundary layer parameterization, Rev. Geophys., 32(4), 363–403, https://dx.doi.org/10.1029/94RG01872, 1994.

Large, W. G. and Pond, S.: Sensible and latent heat flux measurements over the ocean, J. Phys. Oceanogr., 12, 464–482, https://doi.org/10.1175/1520-0485(1982)012<0464:SALHFM>2.0.CO;2, 1982.

Lei, Y., Yao, T., Bird, B. W., Yang, K., Zhai, J., and Sheng, Y.: Coherent lake growth on the central Tibetan Plateau since the 1970s: Characterization and attribution, J. Hydrol., 483, 61–67, https://dx.doi.org/10.1016/j.jhydrol.2013.01.003, 2013.

~~Lewis, W. M.: The thermal regime of Lake Lanao (Philippines) and its theoretical implications for tropical lakes, Limnol. Oceanogr., 18(2), 200-217, https://dx.doi.org/10.4319/lo.1973.18.2.0200, 1973.~~

Li, X., Chao, Y., ~~Mcwilliams~~McWilliams, J. C., and Fu, L. L.: A comparison of two vertical-mixing schemes in a Pacific Ocean General Circulation Model, J. Climate, 14~~(7)~~, 1377–~~-~~1398, https://dx.doi.org/10.1175/1520-0442(2001)014%3C1377:ACOTVM%3E2.0.CO;2, 2001.

~~Liu, M., Zhang, Y., Shi, K., Zhu, G., Wu, Z., Liu, M., and Zhang, Y.: Thermal stratification dynamics in a large and deep subtropical reservoir revealed by high-frequency buoy data, Sci. Total Environ., 651, 614-624, https://dx.doi.org/10.1016/j.scitotenv.2018.09.215, 2019.~~

Lofgren, B. M.: A model for simulation of the climate and hydrology of the Great Lake basin, J. Geophys. Res., 109~~(D18)~~, https://dx.doi.org/10.1029/2004JD004602, 2004.

Long, Z., Perrie, W., Gyakum, J., Caya, D., and Laprise, R.: Northern lake impacts on local seasonal climate, J. Hydrometeorol., 8~~(4)~~, 881–~~-~~896, https://dx.doi.org/10.1175/JHM591.1, 2007.

Ma, N., Szilagyi, J., Niu, G.-Y., Zhang, Y., Zhang, T., Wang, B., and Wu, Y.: Evaporation variability of Nam Co Lake in the Tibetan Plateau and its role in recent rapid lake expansion, J. Hydrol., 537, 27–35, https://dx.doi.org/10.1016/j.jhydrol.2016.03.030, 2016.

~~MacIntyre, S.: Describing fluxes within lakes using temperature arrays and surface meteorology, SIL Proceedings, 1922-2010, 30(3), 339-344, https://dx.doi.org/10.1080/03680770.2008.11902139, 2008.~~

~~MacIntyre, S., Fram, J. P., Kushner, P. J., Bettez, N. D., O'Brien, W. J., Hobbie, J. E., Kling, G. W., Williamson, C. E., Saros, J. E. G., and Vincent, W. F.: Climate-related variations in mixing dynamics in an Alaskan arctic lake, Limnol. Oceanogr., 54(6_part_2), 2401-2417, , 2009.~~

Mahadevan, A., D'Asaro, E., Lee, C., and Perry, M. J.: Eddy-driven stratification initiates North Atlantic spring phytoplankton blooms, Science, 337, 54–~~-~~58, https://dx.doi.org/10.1126/science.1218740, 2012.

Marshall, B. E., Ezekiel, C. N., Gichuki, J., Mkumbo, O. C., Sitoki, L., and Wanda, F.: Has climate change disrupted stratification patterns in Lake Victoria, East Africa? Afr. J. Aquat. Sci., 38(3), 249‒–253, https://dx.doi.org/10.2989/16085914.2013.810140, 2013.

Martynov, A., Sushame, L., and Laprise, R.: Simulations of temperate freezing lakes by one-dimensional lake models: Performance assessment for interactive coupling with regional claimte models, Boreal Environ. Res., 15(2), 143‒–164, 2010.

Michalski, J., and Lemmin, U.: Dynamics of vertical mixing in the hypolimnion of a deep lake: Lake Geneva, Limnol. Oceanogr., 40(4), 809-8–16, https://dx.doi.org/10.4319/lo.1995.40.4.0809, 1995.

Mironov, D. V.: Parameterization of lakes in numerical weather prediction. Description of a lake model, COSMO Technology Report 11[R], Deutscher Wetterdienst, Offenbach am Main, Germany, 2008.

Monin, A. S., and Obukhov, A. M.: Basic laws of turbulent mixing in the atmospheric near the ground, Akad. Naud. SSSR Geofiz. Inst., 24(151), 163‒–187, 1954.

O'Brien, W. J., Barfield, M., Bettez, N., Hershey, A. E., Hobbie, J. E., Kipphut, G., Kling, G., and Miller, M. C.: Long-term response and recovery to nutrient addition of a partitioned arctic lake, Freshwater Biol., 50, 731–741, https://doi.org/10.1111/j.1365-2427.2005.01354.x, 2005.

Oleson, K., Lawrence, D. M., Bonan, G. B., Drewniak, B., Huang, M., Koven, C. D., Levis, S., Li, F., Riley, W. J., Subin, Z. M., Swenson, S., Thornton, P. E., Bozbiyik, A., Fisher, R., Heald, C. L., Kluzek, E., Lamarque, J. F., Lawrence, P. J., Leung, L. R., Lipscomb, W., Muszala, S. P., Ricciuto, D. M., Sacks, W. J., Sun, Y., Tang, J., and Yang, Z.: Technical description of version 4.5 of the Community Land Model (CLM), NCAR Technical Note NCAR/TN-503CSTR, 420 pp., https://doi.org/10.5065/D6RR1W7M, 2013.

Patterson, J. C., Hamblin, P. F., and Imberger, J.: Classification and dynamic simulation of the vertical density structure of lakes, Limnol. Oceanogr., 29(4), 845-861, https://dx.doi.org/10.4319/lo.1984.29.4.0845, 1984.

Perroud, M., Goyette, S., Martynov, A., Beniston, M., and Anneville, O.: Simulation of multiannual thermal profiles in deep Lake Geneva: A comparison of one-dimensional lake models, Limnol. Oceanogr., 54(5), 1574‒–1594, https://dx.doi.org/10.4319/lo.2009.54.5.1574, 2009.

Peters, H., Gregg, M. C., and Sanford, T. B.: On the parameterization of equatorial turbulence: Effect of fine-scale variations below the range of the diurnal cycle, J. Geophys. Res., 100(C9), 18333‒–18348, https://dx.doi.org/10.1029/95JC01513, 1995.

Ping, C. L., Bockheim, J. G., Kimble, J. M., Michaelson, G. J., and Walker, D. A: Characteristics of cryogenic soils along a latitudinal transect in arctic Alaska, J. Geophys. Res., 103, 28917–28928, https://dx.doi.org/10.1029/98JD02024, 1998.

Powell, T., and Jassby, A.: The estimation of vertical eddy diffusivities below the thermocline in lakes, Water Resour. Res., 10(2), 191–198, https://dx.doi.org/10.1029/WR010i002p00191, 1974.

Roekel, L. P. V., Adcroft, A. J., Danabasoglu, G., Griffies, S. M., Kauffman, B., Large, W., Levy, M., Reichl, B., Ringler, T., and Schmidt, M.: The KPP boundary layer scheme: Revisiting its formulation and benchmarking one-dimensional ocean simulations relative to LES, J. Adv. Model. Earth Sy., 10(11), 2647–-2685, https://dx.doi.org/10.1029/2018MS001336, 2018.

Rouse, W. R., Blanken, P. D., Bussières, N., Walker, A. E., Oswald, C. J., Schertzer, W. M., and Spence, C.: An investigation of the thermal and energy balance regimes of Great Slave and Great Bear Lakes, J. Hydrometeorol., 9, 1318–1333, https://dx.doi.org/10.1175/2008JHM977.1, 2008.

Rouse, W. R., Oswald, C. J., Binyamin, J., Spence, C., Schertzer, W. M., Blanken, P. D., Bussieres, N., and Duguay, C. R.: The role of northern lakes in a regional energy balance, J. Hydrometeorol., 6(3), 291–-305, https://dx.doi.org/10.1175/JHM421.1, 2005.

Rouse, W. R., Blanken, P. D., Bussières, N., Walker, A. E., Oswald, C. J., Schertzer, W. M., and Spence, C.: An investigation of the thermal and energy balance regimes of Great Slave and Great Bear Lakes, J. Hydrometeorol., 9(6), 1318-1333, https://dx.doi.org/10.1175/2008JHM977.1, 2008.

Saber, A., James, D. E., and Hayes, D. F.: Effects of seasonal fluctuations of surface heat flux and wind stress on mixing and vertical diffusivity of water column in deep lakes, Adv. Water Resour., 119, 150-163, https://dx.doi.org/10.1016/j.advwatres.2018.07.006, 2018.

Samuelsson, P., Kourzeneve, E., and Mironov, D.: The impact of lakes on the European climate as simulated by a regional climate model, Boreal Environ. Res., 15(2), 113–-129, 2010.

Savtchenko, A., Ouzounov, D., Ahmad, S., Acker, J., Leptoukh, G., Koziana, J., and Nickless, D.: Terra and Aqua MODIS products available from NASA GES DAAC, Adv. Space Res., 34, 710–714, https://dx.doi.org/10.1016/j.asr.2004.03.012, 2004.

Schneider, P., Hook, S. J., Radocinski, R. G., Corlett, G. K., Hulley, G. C., Schladow, S. G., and Steissberg, T. E.: Satellite observations indicate rapid warming trend for lakes in California and Nevada, Geophys. Res. Lett., 36, L22402, https://dx.doi.org/10.1029/2009GL040846, 2009.

Shchepetkin, A. F., and McwilliamsMcWilliams, J. C.: The regional oceanic modeling system (ROMS): A split-explicit, free-surface, topography-following-coordinate oceanic model, Ocean Model., 9(4), 347–-404, https://dx.doi.org/10.1016/j.ocemod.2004.08.002, 2005.

Shimoda, Y., Azim, M. E., Perhar, G., Ramin, M., Kenney, M. A., Sadraddini, S., Gudimov, A., and Arhonditsis, G. B.,.: Our current understanding of lake ecosytem response to climate change: What have we really learned from the north temperate deep lakes? J. Great Lakes Res., 37(1), 173–-193, https://dx.doi.org/10.1016/j.jglr.2010.10.004, 2011.

Stanichny, S. V., Kubryakov, A. A., and Soloviev, D. M.: Parameterization of surface wind-driven currents in the Black Sea using drifters, wind, and altimetry data, Ocean Dynam., 66(1), 1–10, https://dx.doi.org/10.1007/s10236-015-0901-3, 2016.

Stepanenko, V., Jöhnk, K. D., Machulskaya, E., Perroud, M., Subin, Z., Nordbo, A., Mammarella, I., and Mironov, D.: Simulation of surface energy fluxes and stratification of a small boreal lake by a set of one-dimensional models, Tellus A, 66(1), 21389, https://dx.doi.org/10.3402/tellusa.v66.21389, 2014.

Stepanenko, V., Mammarella, I., Ojala, A., Miettinen, H., Lykosov, V., and Vesala, T.: LAKE 2.0: A model for temperature, methane, carbon dioxide and oxygen dynamics in lakes, Geosci. Model Dev., 9~~(5)~~, 1977–~~-~~2006, https://dx.doi.org/10.5194/gmd-9-1977-2016, 2016.

Stepanenko, V. M., Goyetter, S., Martynov, A., Perroud, M., Fang, X., and Mironov, D.: First steps of a Lake Model Intercomparison Project LakeMIP, Boreal Environ. Res., 15~~(2)~~, 191–~~-~~202, 2010.

Stepanenko, V. M., Martynov, A., Jöhnk, K. D., Subin, Z. M., Perroud, M., Fang, X., Beyrich, F., Mironov, D., and Goyette, S.: A one-dimensional model intercomparison study of thermal regime of a shallow turbid midlatitude lake, Geosci. Model Dev. Discuss., 5~~(4)~~, 3993–~~-~~4035, https://dx.doi.org/10.5194/gmdd-5-3993-2012, 2012.

Subin, Z. M., Riley, W. J., and Mironov, D.: An improved lake model for climate simulations: Model structure, evaluation, and sensitivity analyses in CESM1, J. Adv. Model. Earth Sy., 4, https://dx.doi.org/10.1029/2011MS000072, 2012.

Sun, X., Xie, L., Semazzi, F., and Liu, B.: Effect of lake surface temperature on the spatial distribution and intensity of the precipitation over the Lake Victoria basin, Mon. Weather Rev., 143~~(4)~~, 1179–~~-~~1192, https://dx.doi.org/10.1175/MWR-D-14-00049.1, 2015.

Sweers, H. E.: Vertical diffusivity coefficient in a thermocline, Limnol. Oceanogr., 15~~(2)~~, 273–~~-~~280, https://dx.doi.org/10.4319/lo.1970.15.2.0273, 1970.

Thiery, W., Davin, E. L., Panitz, H.-J., Demuzere, M., Lhermitte, S., and van Lipzig, N.: The impact of the African Great Lakes on the regional climate, J. Climate, 28~~(10)~~, 4061–~~-~~4085, https://dx.doi.org/10.1175/JCLI-D-14-00565.1, 2015.

Thorpe, S. A., and Jiang, R.: Estimating internal waves and diapycnal mixing from conventional mooring data in a lake, Limnol. Oceanogr., 43~~(5)~~, 936–~~-~~945, https://dx.doi.org/10.4319/lo.1998.43.5.0936, 1998.

Verhagen, Jan H. G.: Modeling phytoplankton patchiness under the influence of wind-driven currents in lakes, Limnol. Oceanogr., 39, 1551-1565, https://dx.doi.org/10.4319/lo.1994.39.7.1551, 1994.

Wan, Z., Zhang, Y., Zhang, Q., and Li, Z. L.: Quality assessment and validation of the MODIS global land surface temperature, Int. J. Remote Sens., 25, 261–274, https://dx.doi.org/10.1080/0143116031000116417, 2010.

Wang, J., Zhu, L., Daut, G., Ju, J., Lin, X., Wang, Y., and Zhen, X.: Investigation of bathymetry and water quality of Lake Nam Co, the largest lake on the central Tibetan Plateau, China, Limnology, 10, 149–158, https://dx.doi.org/10.1007/s10201-009-0266-8, 2009.

Wang, X., Yi, C., Zhang, H., Farrara, J., Li, Z., Xin, J., Park, K., Colas, F., ~~Mcwilliams~~McWilliams, J. C., and Paternostro, C.: Modeling tides and their influence on the circulation in Prince William Sound, Alaska, Cont. Shelf Res., 63~~(4)~~, S126–~~-~~S137, https://dx.doi.org/10.1016/j.csr.2012.08.016, 2013.

Wu, J.: Wind-induced drift currents, J. Fluid Mech, 68~~(1)~~, 49–~~-~~70, https://dx.doi.org/10.1017/S0022112075000687, 1975.

Xu, L., Liu, H., Du, Q., and Lei, W.: Evaluation of the WRF-lake model over a highland freshwater lake in southwest China: Evaluation of the WRF-lake model, J. Geophys. Res. Atmos., 121(23), 13,989-914,005, https://dx.doi.org/10.1002/2016JD025396, 2016.

Yang, P., Xing, Z., Fong, D. A., Monismith, S. G., Tan, K. M., and Lo, E. Y. M.: Observations of vertical eddy diffusivities in a shallow tropical reservoir, J. Hydro-environ. Res., 9(3), 441-451, https://dx.doi.org/10.1016/j.jher.2014.09.004, 2015.

Yao, H., Samal, N. R., Joehnk, K. D., Fang, X., Bruce, L. C., Pierson, D. C., Rusak, J. A., and James, A.: Comparing ice and temperature simulations by four dynamic lake models in Harp Lake: Past performance and future predictions, Hydrol. Processes, 28(16), 4587–4601, https://dx.doi.org/10.1002/hyp.10180, 2014.

Zhang, G., Yao, T., Xie, H., Qin, J., Ye, Q., Dai, Y., and Guo, R.: Estimating surface temperature changes of lakes in the Tibetan Plateau using MODIS LST data, J. Geophys. Res.-Atmos., 119, 8552–8567, https://dx.doi.org/10.1002/2014JD021615, 2014.

Zhang, Q., Jin, J., Zhu, L., and Lu, S.: Modelling of water surface temperature of three lakes on the Tibetan Plateau using a physically based lake model, Atmos.-Ocean, 56(4), 289–295, https://dx.doi.org/10.1080/07055900.2018.1474085, 2018.

Zhu, L., Jin, J., Liu, X., Tian, L., and Zhang, Q.: Simulations of the impact of lakes on local and regional climate over the Tibetan Plateau, Atmos.-Ocean, 56(4), 230–239, https://dx.doi.org/10.1080/07055900.2017.1401524, 2017.

Zhu, L., Xie, M., and Wu, Y.: Quantitative analysis of lake area variations and the influence factors from 1971 to 2004 in the Nam Co basin of the Tibetan Plateau, Chin. Sci. Bull., 55, 1294–1303, https://dx.doi.org/10.1007/s11434-010-0015-8, 2010.

Figures

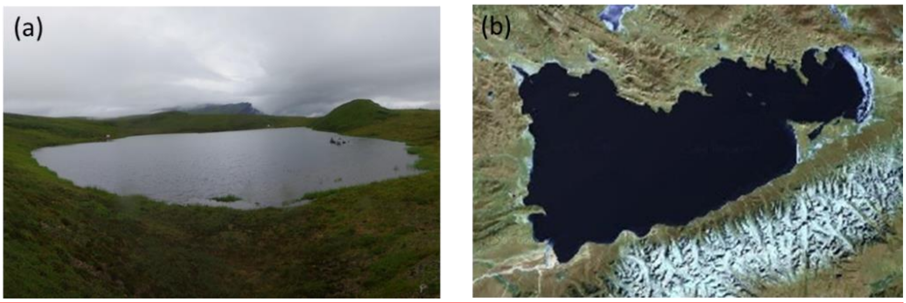

Figure 1. (a) Fog 3 Lake and (b) Nam Co.

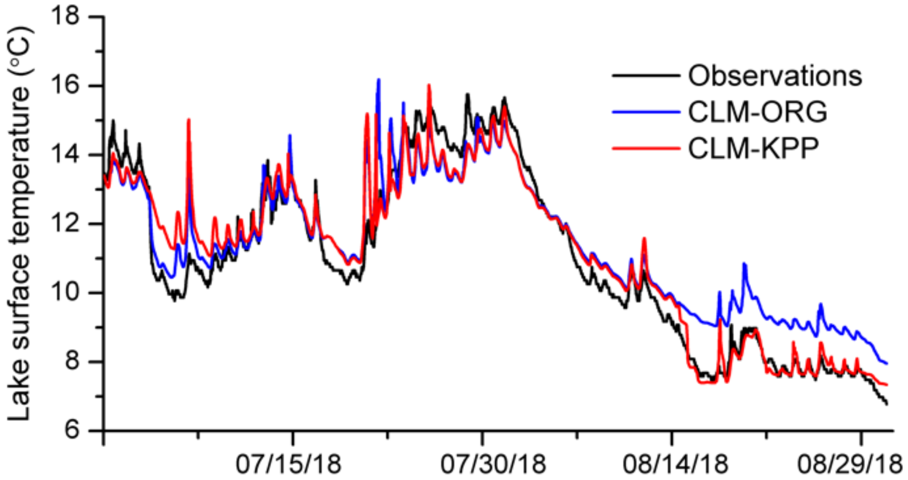

Figure 2. WST observations (black line) and simulations with CLM-ORG (blue line) and CLM-KPP (red line) (unit: ˚C).

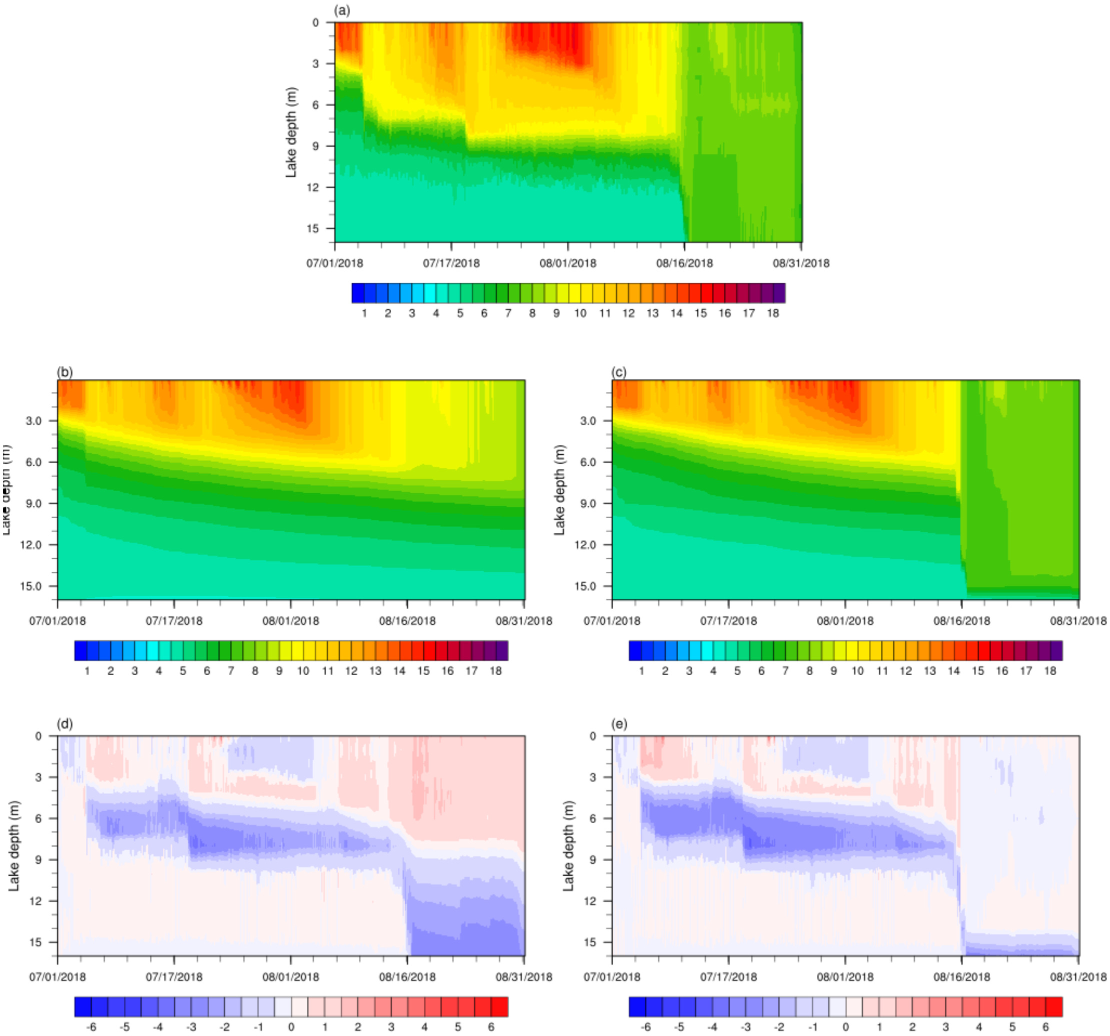

Figure 3. Lake temperature profiles of (a) observations and simulations with (b) CLM-ORG and (c) CLM-KPP. Lake temperature profile differences between simulations and observations (d) CLM-ORG minus observations and (e) CLM-KPP minus observations (unit: ˚C).

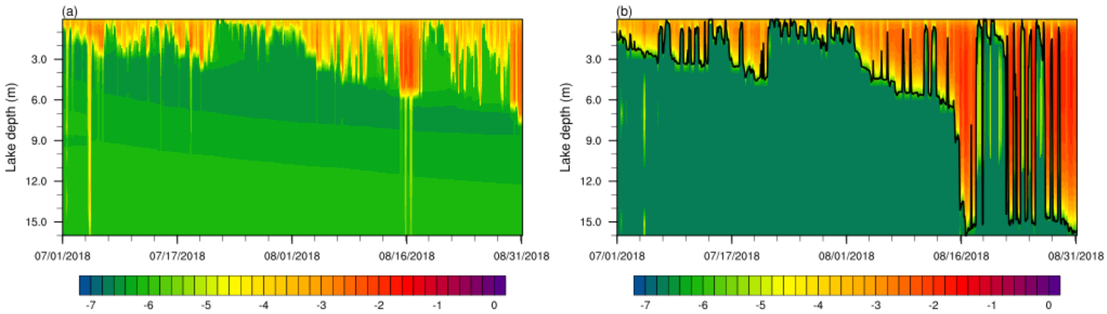

Figure 4. Simulated (a) $log_{10} K_w^{ORG}$ with CLM-ORG, (b) $log_{10} K_w^{KPP}$ with CLM-KPP (Unit: m^2 s^{-1})~~Simulated diffusivity for (a) CLM-ORG and (b) CLM-KPP on a logarithmic scale (Unit: m^2/s)~~. The black line in (b) shows the lake boundary layer depth (Unit: m).

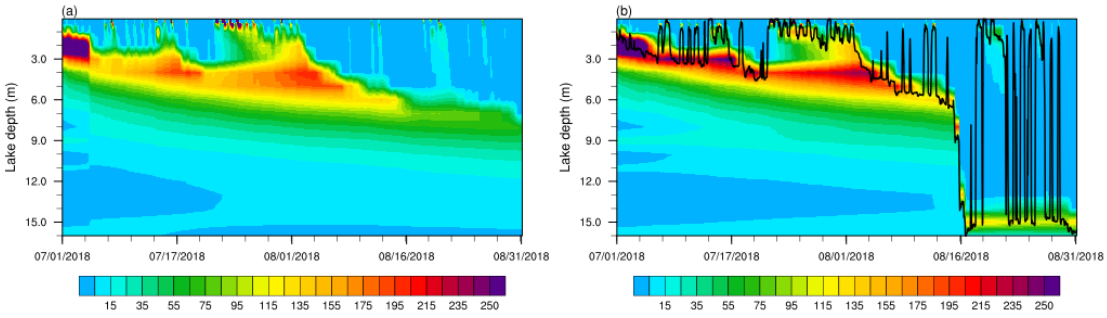

Figure 5. Simulated ~~N~~ N^2 ~~2~~ with (a) CLM-ORG and (b) CLM-KPP (Unit: 10^{-5} ~~/~~ s^{-2}). The black line in (b) shows the lake boundary layer depth (Unit: m).

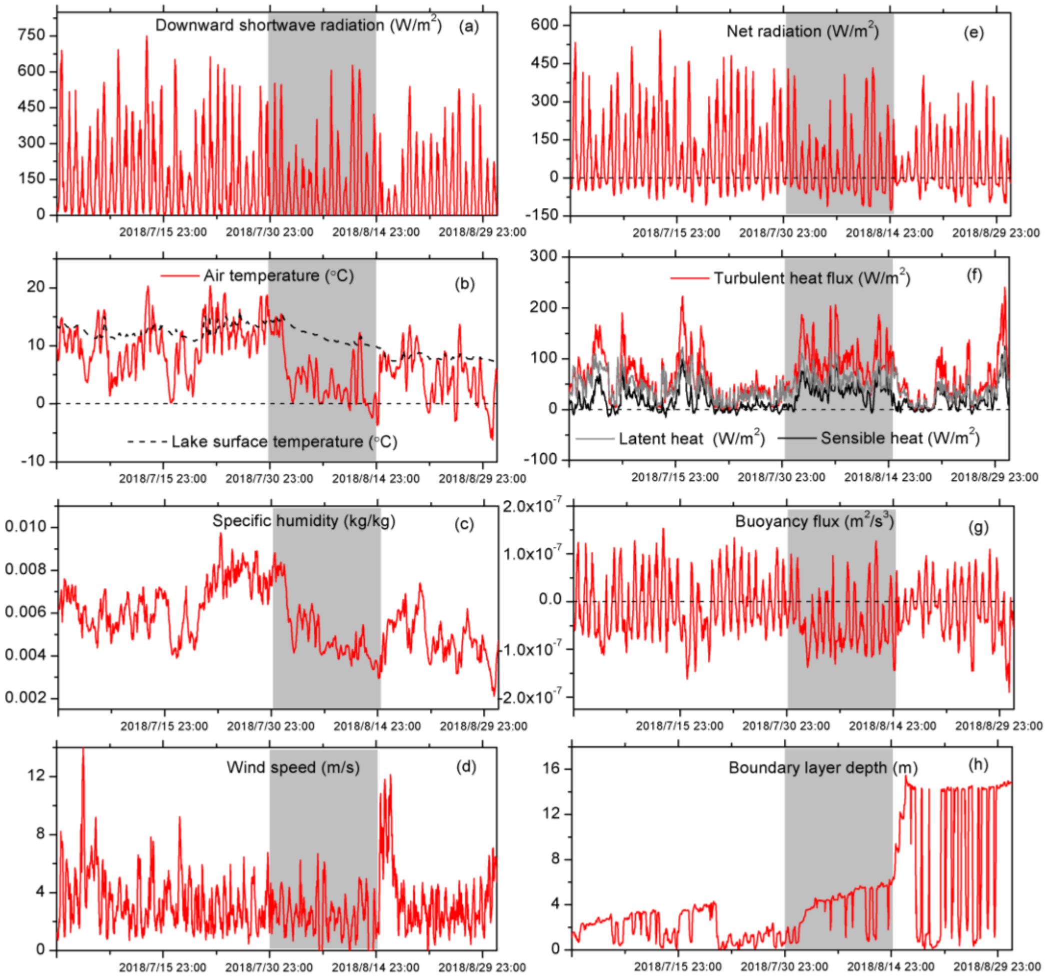

Figure 6. Time series of (a) observed downward shortwave radiation (W m^{-2}), (b) observed air temperature and WST (°C), (c) observed specific humidity (kg kg^{-1}), (d) observed wind speed (m s^{-1}), (e) simulated net radiation (W m^{-2}), (f) simulated turbulent heat flux (W m^{-2}) (red line) with latent heat flux (gray line) and sensible heat flux (black line), (g) simulated buoyancy flux (m^2 s^{-3}), and (h) simulated boundary layer depth (m). The gray shading covers 1 August through 15 August. The simulations were from CLM-KPP.

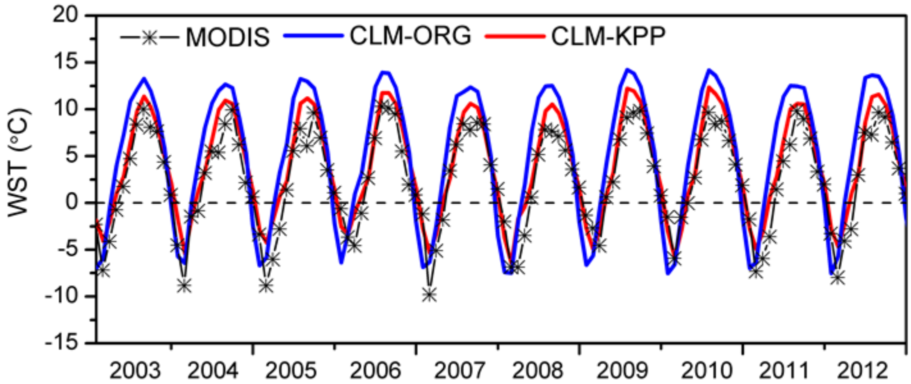

Figure 7. Time series over the period of 2003 through 2012 of monthly WST observations from MODIS (black starred line) and simulations with CLM-ORG (blue line) and CLM-KPP (red line) (Unit: °C).

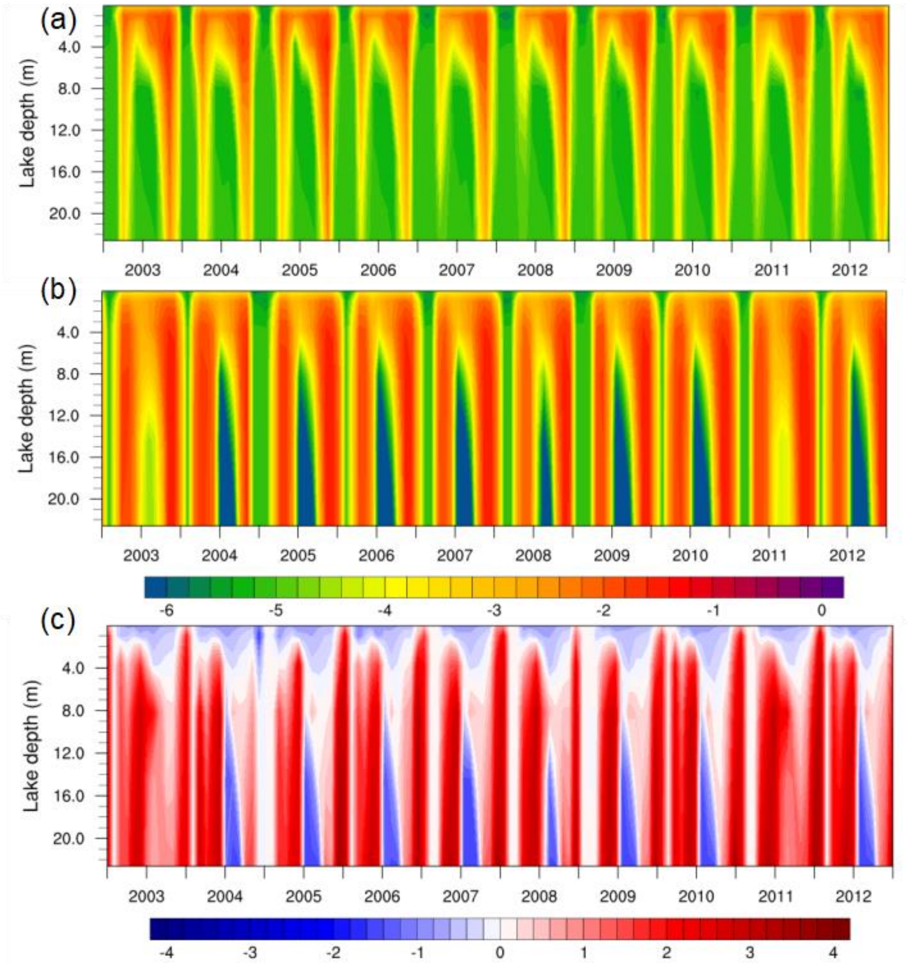

Figure 8. Simulated (a) $log_{10}\,K_w^{ORG}$ with CLM-ORG, (b) $log_{10}\,K_w^{KPP}$ with CLM-KPP (Unit: $m^2\ s^{-1}$) averaged over water columns with depth greater than 25 m (28 of 34 grid cells), and (c) differences between $log_{10}\,K_w^{KPP}$ and $log_{10}\,K_w^{ORG}$ ($log_{10}K_w^{KPP} - log_{10}K_w^{ORG}$).

Table

Table ~~R~~1. RMSE (˚C) and R of temperature profile simulations with CLM-ORG and CLM-KPP for Fog3 Lake for the ~~three~~periods of 1 July–~~through~~ 15 August ~~,~~ and 16–31 August~~,~~ ~~and 1 July through 31 August~~ 2018.

	1 July–15 August, 2018		16–31 August, 2018	
	RMSE (˚C)	R	RMSE (˚C)	R
CLM-ORG	1.1	0.93	1.4	0.57
CLM-KPP	1.3	0.92	0.3	0.99